

1 Compound soil and atmospheric drought events and CO₂ fluxes 2 of a mixed deciduous forest: Occurrence, impact, and temporal 3 contribution of main drivers

4 Liliana Scapucci^{1,*}, Ankit Shekhar^{1,*}, Sergio Aranda-Barranco², Anastasiia Bolshakova³, Lukas
5 Hörtnagl¹, Mana Gharun⁴, Nina Buchmann¹

6 ¹ Department of Environmental Systems Science, ETH Zürich, Switzerland

7 ² Department of Ecology, University of Granada, Granada, Spain

8 ³ University of Natural Resources and Life Sciences, Vienna (BOKU), ~~Austri~~Austria

9 ⁴ Department of Geosciences, University of Münster, Germany

10 *Correspondence to: Liliana Scapucci (liliana.scapucci@usys.ethz.ch)

11 *Both the authors contributed equally to the manuscript

12 **Abstract.** With global warming, forests are facing an increased exposure to compound soil and atmospheric drought (CSAD)
13 events, characterized by low soil water content (SWC) and high vapor pressure deficit (VPD). Such CSAD events trigger
14 responses in both ecosystem and forest floor CO₂ fluxes, of which we know little about. In this study, we used multi-year daily
15 and daytime above-canopy (18 years; 2005-2022) and daily forest floor (five years; 2018-2022) eddy-covariance CO₂ fluxes
16 of a Swiss forest site (montane mixed deciduous forest; CH-Lae). The objectives were (1) to characterize CSAD events at CH-
17 Lae; (2) to quantify the impact of CSAD events on ecosystem and forest floor daily CO₂ fluxes; and (3) to identify the major
18 drivers and their temporal contributions to changing ecosystem and forest floor CO₂ fluxes during CSAD events and CSAD
19 growing seasons. Our results showed that the growing seasons of 2015, 2018, and 2022, were the top three driest ~~at CH-Lae~~
20 ~~since 2005~~ (referred to as CSAD years) ~~at CH-Lae since 2005~~, with similar intensity and duration of the respective CSAD
21 events, but ~~with~~ considerably different pre-drought conditions. The CSAD events reduced daily mean net ecosystem
22 productivity (NEP) in all three CSAD years ~~by about 38% compared to the long-term mean~~, with ~~the~~ highest reduction during
23 2022 (~~30% decrease~~ 41%). This reduction in daily mean NEP was largely due to decreased gross primary productivity (GPP;
24 ~~>15% decrease~~ 16% ~~compared to the long-term mean~~) rather than increased ecosystem respiration (Reco) during CSAD events.
25 Furthermore, forest floor respiration (Rff) decreased during the CSAD events in 2018 and 2022 (no measurements in 2015),
26 with a larger reduction in 2022 (~~⇒40(41%)~~) than in 2018 (~~←25(16%)~~) compared to the long-term mean (2019-2021). Using data-
27 driven machine learning methods, we identified the major drivers of NEP and Rff during CSAD events. While daytime mean
28 NEP (~~NEP_{DT}~~) during 2015 and 2018 CSAD events was limited by VPD or SWC, respectively, ~~daytime-mean-NEP~~ ~~NEP_{DT}~~
29 during the 2022 CSAD event was strongly limited by both SWC and VPD. Air temperature ~~always~~ had ~~always~~ negative effects,
30 ~~while~~ net radiation ~~showed~~ positive effects on ~~daytime-mean-NEP~~ ~~NEP_{DT}~~ during all CSAD events. Daily mean Rff during the
31 2018 CSAD event was driven by soil temperature and SWC, but severely limited by SWC during the 2022 CSAD event. We

Formatted: Font: 17 pt

Formatted: Font: 17 pt

Formatted: MS title

Formatted: Left

Formatted: English (United Kingdom)

32 found that a multi-layer analysis of CO₂ fluxes in forests is necessary to better understand forest responses to CSAD events,
33 particularly if the first signs ~~we saw~~ of NEP acclimation to ~~such~~ CSAD events - ~~we saw~~ for our forest - ~~are~~ found elsewhere
34 as well. We conclude that ~~such~~ CSAD events have multiple drivers with different temporal contributions, making
35 ~~prediction~~ predictions of site-specific CSADs and forest long-term responses to such conditions more challenging.

36 1 Introduction

37 Forests play an essential role in mitigating climate change thanks to their ability to partially offset anthropogenic CO₂ emissions
38 (Harris et al., 2021). However, the increasing frequency of droughts and heatwaves is compromising the carbon uptake capacity
39 of forests worldwide (Anderegg et al., 2022). According to IPCC (2022), the temperature increase over Europe (1850-1990)
40 has been about twice the global mean since the pre-industrial period, accompanied with an increase in frequency of drought
41 events (Spinoni et al., 2018). Recent studies have revealed that European forests are showing increasing rates of tree mortality,
42 induced by low soil water content (SWC) (George et al., 2022). In addition, recent studies have highlighted the role of high
43 vapor pressure deficit (VPD), an indicator of atmospheric drought and a distinct characteristic of heatwaves, ~~in~~ further
44 exacerbating tree mortality (Birami et al., 2018; Gazol and Camarero, 2022; Grossiord et al., 2017, 2020). Due to enhanced
45 land-atmosphere feedback ~~due~~ in response to climate change, the frequency of ~~co-occurrence of~~ occurring low soil moisture
46 and high VPD conditions has also increased (Dirmeyer et al., 2021; Miralles et al., 2019; Orth 2021; Zhou et al., 2019),
47 resulting in so-called compound soil and atmospheric drought (CSAD) conditions. The 21st century European droughts in
48 2003, 2015, 2018, and the most recent one in 2022, were indeed characterized by CSAD conditions (Dirmeyer et al., 2021;
49 Ionita et al., 2021, 2017; Lu et al., 2023; Tripathy and Mishra, 2023). In 2022, Europe experienced its hottest and driest year
50 on record, with the summer being the warmest ever recorded, which ultimately led to numerous CSAD events across the
51 continent (Copernicus Climate Change Service, 2023).

52 Such CSAD events have multiple impacts on forest ecosystems. They can lead to reduced net ecosystem productivity (NEP)
53 by decreasing gross primary productivity (GPP) and/or increasing ecosystem respiration (Reco) (Xu et al., 2020). Additionally,
54 soil respiration (SR) can be reduced due to water scarcity in the soil, which limits both heterotrophic and autotrophic respiration
55 (Ruehr and Buchmann, 2009; Ruehr et al., 2010; van Straaten et al., 2011; Sun et al., 2019; Schindlbacher et al., 2012).
56 ~~Still~~ However, high soil temperature (TS) can increase SR rates when soil moisture is not limiting metabolic reactions in the
57 soil (Schindlbacher et al., 2012), affecting the sensitivity of respiration to soil temperature (Sun et al., 2019). Thus, to better
58 understand the ecological consequences of climate change on forest ecosystems, the capacity of forests to acclimate to stress
59 conditions like CSAD events, e.g., by changing the NEP sensitivity to abiotic drivers like air temperature (Tair), VPD, and
60 SWC during a growing season or among growing seasons, needs to be known (Grossman, 2023).

61 The summer of 2022 in Europe, characterized by strong CSAD conditions (Tripathy and Mishra, 2023; van der Woude et al.,
62 2023), showed an extensive reduction in forest greenness (about 30% of temperate and Mediterranean European forest area;
63 Hermann et al., 2023), and a reduction in GPP (van der Woude et al., 2023), comparable to summer 2018 CSAD events. In

64 2018, this resulted in drought-induced tree mortality in Scots pine (*Pinus sylvestris* L.) and European beech (*Fagus sylvatica*
65 L.) forests (Haberstroh et al., 2022; Obladen et al., 2021; Rukh et al., 2023; Schuldt et al., 2020). Clearly, most drought impact
66 studies use data measured above the canopy, ~~be-iti.e.~~, net carbon dioxide (CO₂) exchange or remote sensing of vegetation;
67 ~~particular.~~ Particularly the latter is largely neglecting the below-~~canopy~~ component of the forest (also known as forest floor),
68 ~~while~~ although it might show contrasting responses to drought conditions compared to the top canopy sensed from above (Chi
69 et al., 2021). The forest floor, composed of soil, tree roots, woody debris, and understory vegetation, provides an essential
70 interface for soil-atmosphere CO₂ exchange, with photosynthesis of understory vegetation and forest floor respiration (Rff),
71 both representing major CO₂ exchange ~~pathways~~ processes (Chi et al., 2017; Paul-Limoges et al., 2017). Therefore, separating
72 the ecosystem-level drought response from the forest floor drought response provides a more comprehensive insight into
73 drought impacts than one level alone (Chi et al., 2017; Martinez-Garcia et al., 2022). Furthermore, the intensity and duration
74 of CSAD events, and their impacts on forests can largely vary at regional scale (Pei et al., 2013; Kim et al., 2020). Thus, more
75 attention is needed on temperate forest ecosystems across Central Europe, such as in Switzerland, where forests are accustomed
76 to humid and cool climates, with ample amount of summer rainfalls (Schuldt and Ruehr, 2022).
77 In Switzerland, 2022 was the warmest year on record since the beginning of instrumental measurements in 1864, with average
78 air temperatures 1.6 °C above the long-term mean (1991-2020), and annual precipitation amounting to only 60% of the long-
79 term average (MeteoSvizzera, 2023). Such hot and dry conditions as in 2022 were bound to result in CSAD events which
80 could ultimately compromise the ~~carbon dioxide~~ CO₂ uptake capacity of forests. Thus, the objectives of this study were as
81 follows: (1) to characterize compound soil and atmospheric drought (CSAD) events at a Swiss montane mixed deciduous
82 forest site, (2) to quantify the impact of CSAD events on ecosystem and forest floor CO₂ fluxes, and (3) to identify the major
83 drivers of ecosystem and forest floor CO₂ fluxes and their temporal contributions during CSAD events and CSAD growing
84 seasons.

85 2 Material and methods

86 2.1 Forest site

87 The study was conducted in a managed mixed deciduous mountain forest (CH-Lae at 682 m a.s.l.) located at the Lägeren, in
88 the far east of the Jura Mountain range in Switzerland. The CH-Lae forest has a complex canopy structure with a rather high
89 species diversity, the dominant species are European beech (*Fagus sylvatica*; L., 40% cover), ash (*Fraxinus excelsior*; L., 19%
90 cover), Sycamore maple (*Acer pseudoplatanus*; L., 13% cover), European silver fir (*Abies alba*; Mill., 8% cover), large-leaved
91 linden (*Tilia platyphyllos*; Scop., 8%) and Norway spruce (*Picea abies*; (L.) H. Karst., 4% cover) (Paul-Limoges et al., 2020);
92 showing no significant trend of leaf area index (LAI) over the years. The soils at CH-Lae are characterized by two main types,
93 rendzic leptosols and haplic cambiosols, with bedrocks of limestone marl, sandstone, and transition zones between the two
94 (Ruehr et al., 2010). The mean annual air temperature at CH-Lae was 8.8 ± 1.3 °C (mean \pm ~~sd~~ SD), and mean annual
95 precipitation was 831 ± 121 mm (mean 2005-2022). The understory vegetation at CH-Lae is dominated by wild garlic (*Allium*

Formatted: Subscript

96 *ursinum*, L., height ~ 30 cm) which grows for a short period in spring and early summer (March-June) (Ruehr and Buchmann,
97 2009). The net carbon uptake period of CH-Lae is from May to September (Figure A1, appendix A).

98 2.2 Ecosystem-level measurements

99 ~~Measurements~~In this study, we used measurements of ecosystem CO₂ fluxes from above the forest canopy using the eddy
100 covariance (EC) technique (Aubinet et al., 2012) started in April 2004. Here we used data (Aubinet et al., 2012), spanning from
101 2005 to 2022 (full years) of net ecosystem productivity (NEP), gross primary productivity (GPP), and ecosystem respiration
102 (Reco). The EC system (eddy tower coordinates: 47°28'42.0" N and 8°21'51.8" E) was mounted at a height of 47 m (mean
103 canopy height of 30 m). We performed above the ground. The EC technique utilizes high frequency (20 Hz) measurements
104 of wind speed and wind direction using, measured with a three-dimensional sonic anemometer, and used gas (here CO₂)
105 concentration, measured with an infrared gas analyser (IRGA) to measure as CO₂ molar density (with an open-path IRGA from
106 2004-2015) or as dry mole fraction (with a closed-path IRGA from 2016-2022; for details of instrumentation used in the EC
107 system, see Table A1, appendix A). The time-lag between turbulent fluctuations of vertical wind speed and CO₂ molar density
108 or dry mole fraction was calculated by covariance maximization (Fan et al., 1990), and (Fan et al., 1990); half-hourly fluxes of
109 CO₂ (F_C, μmol CO₂ m⁻² s⁻¹) were then calculated from the 20 Hz measurements using the EddyPro software v7 (v7.0.9, LI-
110 COR Inc., Lincoln, NE, USA), following established community guidelines (Aubinet et al., 2012; Sabbatini et al., 2018).
111 Fluxes (Aubinet et al., 2012; Sabbatini et al., 2018). The F_C from the open-path IRGA LI-7500 were corrected for air density
112 fluctuations (Webb et al., 1980). Spectral (Webb et al., 1980), all F_C underwent spectral corrections for high-pass (Moncrieff
113 et al., 2004) (Moncrieff et al., 2004) and low-pass filtering (Fratini et al., 2012; (Fratini et al., 2012; Horst, 1997)) losses were
114 applied to the raw fluxes. The impact of self-heating of the open-path IRGA on F_C was corrected following the based on a
115 method described by Kittler et al. (2017). Thereafter, F_C were filtered for turbulent conditions based on the steady state test
116 statistic and integrated turbulence criterion test (Foken et al., 2004). Additional quality control flags (QCF) for each half hourly
117 CO₂ flux were calculated based on Sabbatini et al. (2018); fluxes with QCF=2 (unreliable flux value) were removed. Kittler et
118 al. (2017). The net ecosystem CO₂ exchange (NEE) was then calculated as the sum of F_C and the CO₂ storage term. Thereafter,
119 four quality checks were applied to the calculated NEE, namely (1) despiking using a Hampel filter to reject NEE values higher
120 or lower than five times the standard deviation estimated from the median absolute deviation in a 9 day running window, (2)
121 absolute threshold filtering to remove values outside a physically plausible range concentrations based on 1-point
122 measurements (Greco and Baldocchi, 1996). The quality of -50 to 50 μmol m⁻² s⁻¹, (3) removal of potential non-biotic fluxes
123 during cold season using a trimming mean approach (see Etzold et al., 2011), (4) constant u* (friction velocity) filtering of 0.3
124 ms⁻¹ for CH-Lae (Etzold et al., 2010). Then, the missing half-hourly NEE flux values was ensured by applying a comprehensive
125 quality screening process that combined several well-tested methods into a single quality flag (0-1-2 system; Mauder and
126 filtered NEE time series was Foken, 2006; Sabbatini et al., 2018). Fluxes of low quality (flag = 2) were removed from further
127 analyses. Fluxes that passed the quality-screening process were then gap-filled using the marginal distribution sampling (MDS)
128 approach as implemented in the ReddyProc v1.3.2 R-package (Reichstein et al., 2005; Wutzler et al., 2018). Finally, the gap-

Formatted: Not Superscript/ Subscript

Formatted: Not Superscript/ Subscript

Formatted: Not Superscript/ Subscript

Formatted: Not Superscript/ Subscript

filled NEE was (Reichstein et al., 2005) and partitioned into gross primary productivity (GPP) and ecosystem respiration (Reco) using the day-time partitioning method (Lasslop et al., 2010) (Lasslop et al., 2010). More details about quality-screening, gap-filling and partitioning can be found in Shekhar et al. (2024). In this study, we used net ecosystem productivity (NEP = $-$ NEE) for further data analyses. Positive NEP fluxes represent CO₂ uptake by the forest, whereas negative NEP represent CO₂ release. Along with fluxes, we also measured half-hourly air temperature (T_{air}), relative humidity (RH), incoming short-wave radiation (R_g) and precipitation (Precip) at the top of the EC tower from 2005-2022 (see Table A1 for instrumentation details). We estimated half-hourly VPD from half-hourly measurements of air temperature and relative humidity. For more information about the processing chain refer to Shekhar et al., 2024.

2.3 Forest floor measurements

We measured forest floor fluxes of CO₂ based on the EC technique (Aubinet et al., 2012) below the canopy from 2018 to 2022 to estimate net ecosystem exchange of the forest floor (NEE_{ff}), which includes CO₂ fluxes from the soil and the understory vegetation. We partitioned NEE_{ff} into gross primary productivity of the forest floor (GPP_{ff}) and respiration of the forest floor (R_{ff}; Lasslop et al., 2010). The below-canopy station at CH-Lae site was located in a distance of c. 100 m from the main tower (47°28'42.9" N and 8°21'27.6" E) and had a height of 1.5 m. Wind speed and direction were measured with a sonic anemometer and CO₂ concentrations with an open-path IRGA (LI-7500; Table A1) at a frequency of 20 Hz. We calculated NEE_{ff}, and the partitioned fluxes, using the same process and corrections as for above-canopy measurements (except for the self-heating correction). We used a seasonal u* filtering to account for changes in the understory canopy, with 0.024 ms⁻¹ for spring (day 60-151), 0.027 ms⁻¹ for summer (day 152-243), 0.039 ms⁻¹ for autumn (day 244-334), and 0.025 ms⁻¹ for winter (day 335-60). Additionally, we continuously measured air temperature (T_{air}), relative humidity (RH_{ff}), incoming short-wave radiation (R_g), soil temperature (TS) and soil water content (SWC) at multiple depths 5, 10, 20, 30, 50 cm depth at the forest floor meteorological station next to the below-canopy EC system (Table A1, appendix A). In 2020, we installed an additional soil moisture profile. To account for spatial heterogeneity, we centre-normalised the SWC data and using a z-score transformation, we then used z-scores of SWC for further analyses.

2.4 Soil respiration measurements

Ten PVC collars (diameter 20 cm, height 13 cm, depth = 2 cm) were installed at CH-Lae in spring 2022, at the same locations within the footprint of the tower as described in Ruehr et al. (2010). Soil respiration (SR) measurement campaigns were performed at least once a month from March until November 2022, with a LI-8100-103 analyser and a closed chamber (Table A1, appendix A). Collars were measured once a day in a random order during each campaign. Every measurement lasted 90 seconds from the moment the LI-8100 chamber closed on top of the collar. Next to each collar, we measured SWC_s (SWC from survey measurements) at 5 cm with a soil moisture sensor, and TS_s (TS from survey measurements) at 5 cm with a temperature sensor (Table A1, appendix A). When the Swiss meteorological service (MeteoSwiss) forecasted a two-week heatwave starting on 14th of July 2022, we intensified the measurements of SR to one campaign every second day with two

161 rounds of measurements per day for two weeks (at 09:00 and at 16:00). The order of measurements was inverted every
162 fieldwork day. Since the portable soil moisture sensor broke on 22nd of July 2022 and was only available on 11th of August
163 2022, we calculated the SWC based on continuous measurements at the forest floor meteorological station for these days
164 ($SWCs = 1.34 * SWC - 10.7$; $R^2 = 0.82$).

165 2.5 Data analyses

166 In this study, we focused all our ~~analysis~~analyses on the growing season, between May and September, when the long-term
167 mean of ecosystem NEP (2005-2022) was positive, implying that GPP of the vegetation overcompensated all respiratory losses
168 (Figure A1, ~~appendix A~~; Körner et al., 2023). We conducted all data analyses using ~~the~~ R programming language (R ~~version~~
169 ~~4.3.3~~, R core team, 2021). We compared cumulative precipitation (indicating total water supply to the forest) and cumulative
170 VPD (indicating total atmospheric water demand) during the growing seasons of 18 years at our forest site and chose the three
171 years with the driest growing seasons, i.e., with low cumulative precipitation and high VPD, ~~called compound soil and~~
172 ~~atmospheric drought (CSAD) years hereafter~~. Then, we identified the CSAD events during ~~the~~these CSAD years as periods
173 when both soil and atmosphere were significantly drier than usual for more than 10 consecutive days, implying a compound
174 drought condition. To identify drier than usual periods, we compared 5-day moving daily means (assigned to the centre of 5
175 days) of SWC and VPD with their long-term (2005-2022) means. So, a period of 10 or more consecutive days with SWC being
176 significantly lower ($p < 0.05$) and VPD being significantly higher ($p < 0.05$) than the long-term mean, ~~was~~ identified as
177 CSAD ~~event~~event.

178 We quantified the impact of CSAD events based on anomalies of NEP, GPP, Reco, and Rff by comparing them with their
179 respective long-term means (NEP, GPP, Reco: mean of 2005-2022; Rff: mean of 2019-2021). Since CSAD events occurred
180 in two of the five years of flux data available at the forest floor station (Rff), we excluded 2018 and 2022 from the calculation
181 of ~~the~~ Rff long-term mean. To understand the major drivers of NEP and Rff, we performed two different driver analyses in
182 this study, first focusing on the CSAD years, (I), and second focusing on the CSAD events in the CSAD years, (II).
183 (I) For the first driver analysis, we used the conditional variable importance (CVI) feature based on random forest regression
184 model (Breiman, 2001). For modelling daily mean NEP, (NEP), the predictors were Rg, VPD, and Tair measured above the
185 canopy, and SWC measured at the forest floor station, whereas for modelling daily mean Rff, (Rff), the predictors were Rg
186 (Rg_{ff}) and Tair ($Tair_{ff}$) as well as soil temperature (TS) and SWC, measured at the forest floor station. ~~The model was run for~~
187 ~~each year separately~~. The CVI ~~considers~~is specifically designed to consider the multi-collinearity ~~between the~~among predictors
188 (i.e., Tair, VPD, Rg), while estimating the importance of ~~each~~ predictor ~~variables~~variable (Strobl, et al., 2008), and thus
189 ~~considered a very reliable method to estimate overall feature importance~~. For estimating CVI, we used the *cforest* and *varimp*
190 function from the R-package *party* (Hothorn et al., 2006).

191 (II) For the second driver analysis, we used daytime mean NEP (NEP_{DT} , excluding nighttime data ~~to highlight the effects of~~
192 ~~environmental drivers when photosynthesis is dominating~~) to avoid potential biases if GPP were used, since some predictors,
193 (i.e., Tair and Rg_{ff}) were used ~~for the partitioning of to partition~~ NEE into GPP and Reco. We used a TreeExplainer-based

194 SHapley Additive exPlanations (SHAP) framework (Lundberg and Lee, 2017; Lundberg et al., 2020), with a tree-based
195 ensemble learning extreme gradient boosting (XGB) model (Chen and Guestrin, 2016). The XGB model was used to model
196 ~~daytime mean NEP_{DT} and daily mean Rff~~, applying the GridSearchCV methodology to optimize the parameters of the
197 XGB model for NEP and Rff (see Wang et al., 2022 for more details). The TreeExplainer-based SHAP framework integrates
198 explanatory models (here the XGM model) with game theory (Shapley, 1953), which allowed us to estimate the marginal
199 contribution (known as SHAP value) of each predictor variable (i.e., Tair, VPD, SWC, TS) to ~~predicted~~the response variables-
200 ~~(NEP_{DT}, Rff)~~. We used the function *xgboost* (eXtreme Boosting Training) from the R-package *xgboost* to train the model, and
201 the functions *shap.values* and *shap.prep* from the R-package *SHAPforxgboost* (Chen and Guestrin, 2016) to obtain the SHAP
202 values of each predictor variable for ~~daytime mean NEP_{DT}~~ (for 2005-2022) and ~~daily mean Rff~~ (for 2018-2022). ~~The~~
203 ~~models were run for each year separately, and we obtained the marginal contributions of each feature for each day of each~~
204 ~~growing season, which allowed to observe their temporal course.~~ Then we calculated the mean SHAP value during the CSAD
205 events for each predictor of ~~daytime mean NEP_{DT}~~ and ~~daily mean Rff~~ for the CSAD years. ~~For comparison to determine~~
206 ~~the dominant direction of the effect of each feature. To determine differences to the long-term means,~~ we also calculated the
207 mean SHAP values of the predictors during the respective reference periods (long-term means: 2005-2022 for ~~daytime mean~~
208 ~~NEP_{DT}~~; 2019-2021 for daily Rff). The respective reference period ~~includes~~included all days, in which a CSAD event
209 occurred independent of the year, i.e., ranging from 7th July to 23rd August for ~~daytime mean NEP_{DT}~~ during 2005-2022
210 (including CSAD years due to the large number of years available with measurements), and from 14th July to 23rd August for
211 ~~daily mean Rff~~ during 2019-2021 (excluding CSAD years due to the small number of years available with measurements;
212 Figure A2, ~~appendix A~~)-). ~~For comparison with the first model (based on CVD), we also calculated the mean and standard~~
213 ~~error of the absolute SHAP values for NEP in 2015, 2018, 2022, and the long-term mean 2005-2022 (Figure A3). However,~~
214 ~~since we were interested in the short-term changes in driver importance, including the direction of their effect, we did not~~
215 ~~follow up using absolute SHAP values in this study.~~
216 ~~Moreover, we~~We then used the SHAP values of drivers (VPD, Tair and SWC for ~~NEP_{DT}~~; TS and SWC for Rff) to ~~derive~~
217 ~~driver thresholds, i.e., estimate acclimation of NEP_{DT} and Rff to abiotic drivers by estimating~~ the absolute driver values
218 (thresholds) related to the largest effects, as indicated by ~~highest~~the maximum marginal contributions to the response variables
219 ~~NEP_{DT} and Rff~~ for each CSAD year (Gou et al., 2023; Wang et al., 2022). For this, we fitted a local polynomial regression
220 (~~LOESS curve~~)-between the SHAP values of the driver variable and the driver variable itself, ~~and i.e., a loess curve, and~~
221 ~~calculated the residual standard error from the loess function of the stats R-package.~~ We then identified the absolute driver
222 value corresponding to the highest SHAP value. ~~We specifically derived (feature_NEP_{max}, feature_Rff_{max}) for each CSAD~~
223 ~~year, i.e., VPD_NEP_{max}, Tair_NEP_{max}, SWC_NEP_{max}, i.e., the VPD, Tair and SWC, values~~ associated with the highest marginal
224 contributions to ~~daytime mean NEP, and NEP_{DT}, as well as~~ TS_Rff_{max} and SWC_Rff_{max}, i.e., TS and SWC, values associated
225 with the highest marginal contributions to ~~daily Rff~~. These absolute driver values provided information about the NEP_{DT} and
226 Rff sensitivities to abiotic drivers during the growing season of each CSAD year. For example, a shift in the SWC_NEP_{max}
227 towards drier conditions in one growing season compared to others thus translated to an acclimation of NEP_{DT} to drier

228 conditions in that growing season. To test if the feature NEPmax values varied with the corresponding mean feature values
229 during the respective growing season, we fitted a linear regression between the mean $R\#VPD$, SWC and T_{air} and their
230 corresponding values of NEPmax for each CSAD-year, from 2005 to 2022.

231 Finally, we used linear models to explain daily mean SR responses to TS and SWC during the CSAD events and the rest of
232 the years, based on the measurements from the survey campaigns in 2022. The amount of SR data was not sufficient to use
233 machine learning approaches.

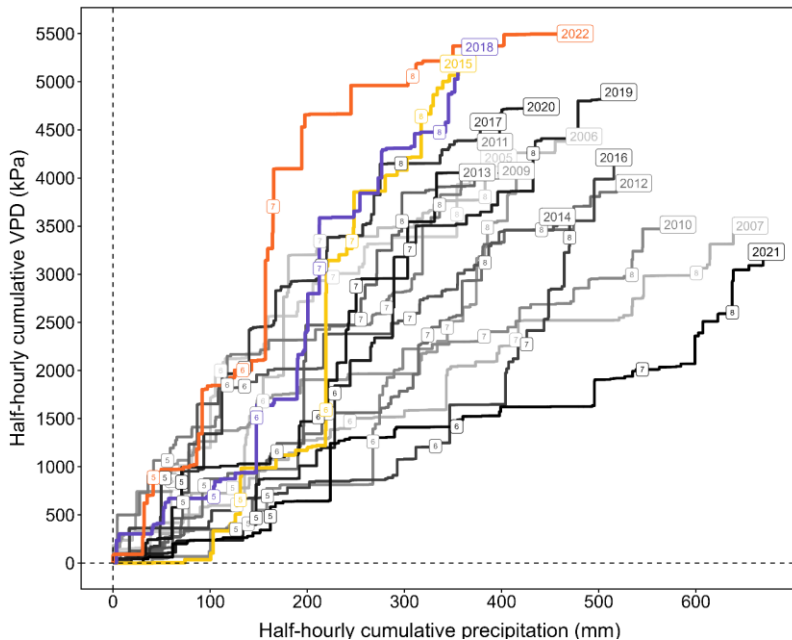
234 3 Results

235 3.1 Detected CSAD events

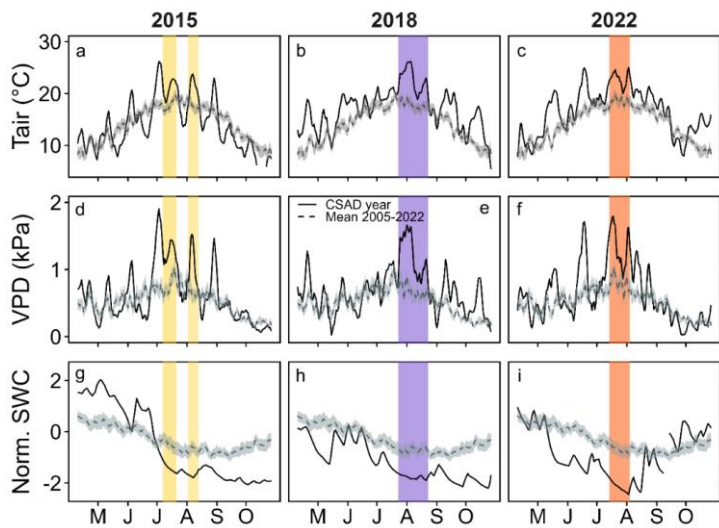
236 The growing seasons (May to September) of 2015, 2018, and 2022 were the three driest in the last 18 years (2005-2022) which
237 the mountain forest site experienced (Figure 1). The growing seasons in these three years were characterized by very high
238 atmospheric drought (indicated by cumulative VPD) and low water supply (indicated by cumulative precipitation, a proxy for
239 soil drought), ~~called compound soil and atmospheric drought (CSAD) years hereafter.~~ In particular, the summer months (June-
240 August) of these three years were significantly warmer and drier (Figures 1, 2). Mean summer temperatures of 2018 (19.8 °C)
241 and 2022 (20.3 °C) were more than 2.5 °C higher than the long-term mean summer temperature at the forest site (17.2 °C);
242 summer precipitation sums in 2018 and 2022 were more than 20% and 10% lower than the long-term mean cumulative summer
243 precipitation (300 mm), respectively. Furthermore, during the month July of both years 2015 and 2022, less than one-third of
244 long-term mean cumulative summer precipitation was recorded. Coupled with a more than 50% increase in average VPD, this
245 resulted in intense soil and atmospheric drought conditions.

246 Moreover, we detected two distinct CSAD events in 2015, i.e., periods of 10 or more consecutive days with significantly lower
247 SWC and significantly higher VPD than the long-term mean: one from 7th July 2015 to 21st July 2015, and a second one from
248 2nd August 2015 to 13th August 2015 (Figure 2a, d, g), comprising a total of ~~25~~27 days with a mean maximum temperature of
249 26.9 °C, mean maximum VPD of 2.24 kPa, and mean minimum normalized SWC of -1.83 (Table 1). For comparison, in 2018,
250 the CSAD event lasted for ~~34~~32 days, from 23rd July 2018 to 23rd August 2018 (Figure 2b, e, h), with a mean maximum
251 temperature of 27.7 °C, mean maximum VPD of 2.19 kPa, and mean minimum normalized SWC of -1.94 (Table 1). In 2022,
252 the CSAD event lasted ~~24~~22 days, from 14th July 2022 to 4th August 2022. Thus, although it was shorter than in those in 2015
253 and 2018 (Figure 2c, f, i), it was more intense than those in 2015 and 2018, with mean maximum temperature of 28.3 °C, mean
254 minimum VPD of 2.43 kPa, and mean minimum normalized SWC of -2.51 (Table 1). We measured the highest air temperature
255 (33.56 °C) and the third highest VPD (3.83 kPa) ever recorded at the forest site in the past 18 years (2005-2022) on the last
256 day of the 2022 CSAD event, i.e., on 4th August 2022 between 16:30 and 17:00 (Figure ~~A3~~, ~~appendix-AA4~~). Furthermore, the
257 2022 CSAD event was characterized by multiple tropical nights (i.e., nighttime temperature > 20 °C; Figure ~~A3~~, ~~appendix~~
258 ~~AA4~~) and progressive soil drying (Figure 2).

259 Thus, the CSAD events were not only slightly different in terms of intensities, but also in terms of time of CSAD occurrence
 260 (Table 1), and initial drought development. In both years 2015 and 2018, wetter (than long-term mean; 2015) or normal (2018)
 261 soil conditions continued from late spring (mid-May) until end of June, with a quick soil drought intensification in July due to
 262 high air temperatures ($> 30^{\circ}\text{C}$), high VPD (>3.8 kPa) (Figure 2), and low precipitation (more than 40% lower than the long-
 263 term July average). The year 2022, however, was already characterized by exceptionally low soil water content and high VPD
 264 (> 2.5 kPa) in May (Figure 2i), which intensified with low precipitation and high temperatures into early summer. Nighttime
 265 VPD exceeded 2 kPa on a few days in June, before the CSAD event occurred mid-July to beginning of August (see Figure A3,
 266 appendix AA4). Even the heavy rainfall on 5th August 2022 (28 mm) only resulted in a minor increase of SWC. Nevertheless,
 267 after 4th August, air temperature and VPD conditions became near-normal, thereby marking the end of the 2022 CSAD event
 268 (Figure 2).



269
 270 **Figure 1. Cumulative VPD and cumulative precipitation from May to September (growing season of the Lägeren forest) of each**
 271 **year (2005-2022). The numbers (5-9) on the cumulative lines depict the end of each month.**



272

273 Figure 2. Comparison of 5 day moving averages of daily mean (a-c) Tair, (d-f) VPD, and (g-i) SWC in the years when a CSAD event
 274 happened against the long-term means (2005-2022). The band around the dashed line indicates the standard error of the long-term
 275 mean 2005-2022. The coloured areas mark the CSAD events, i.e., periods with co-occurring lowest SWC and highest VPD.

276 Table 1. Characterization of CSAD events in 2015, 2018 and 2022. Duration, maximum (Max.) and standard deviation (\pm SD) of
 277 daily mean Tair, maximum (Max.) and standard deviation (\pm SD) of daily mean VPD, and minimum (Min.) and standard deviation
 278 (\pm SD) of daily mean normalized SWC recorded during the CSAD events in 2015, 2018 and 2022 are given.

Year	Duration (days)	Max. \pm SD	Max. \pm SD	Min. \pm SD
		Tair ($^{\circ}$ C)	VPD (kPa)	SWC (normalized)
2015	11+14=25 <u>15+12</u> $\equiv 27$	26.9 \pm 3.03	2.24 \pm 0.4	-1.83 \pm 0.20
2018	34 <u>32</u>	27.7 \pm 2.88	2.19 \pm 0.5	-1.93 \pm 0.10
2022	24 <u>22</u>	28.3 \pm 2.64	2.43 \pm 0.5	-2.51 \pm 0.20

279 3.2 Impacts of CSAD events on CO₂ fluxes

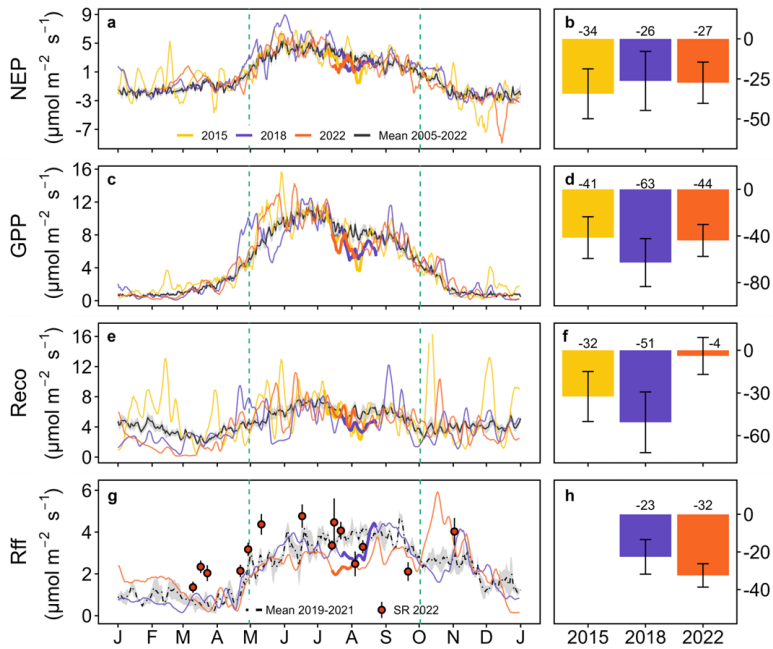
280 All CSAD events had immediate negative impacts on ecosystem CO₂ fluxes, showing a decrease in the CO₂ fluxes compared
 281 to the long-term means (Table 2, Figure 3a, c, e, g). Mean daily NEP, GPP, Reco and Rff tended to be lower during the
 282 CSAD events compared to the respective long-term means of the reference periods 2005-2022 (for NEP, GPP and Reco) and

283 2019-2021 (for Rff; Table 2), with much larger variations during CSAD events compared to those of the reference periods
 284 (except for Rff; Figure 3b, d, f, h). The lowest average NEP was recorded in the CSAD event of 2022, (minus 41%), followed
 285 by NEP in the 2018 and 2015 CSAD events, (minus 38% and minus 35%, respectively), while the lowest average GPP and
 286 Reco were found in the 2018 CSAD event (minus 28% and minus 31%, respectively; Table 2).

287 All cumulative CO₂ fluxes decreased during CSAD events in 2015, 2018 and 2022 compared to the long-term means (Figure
 288 3b, d, f, h), with the only exception of Reco in 2022. The cumulative NEP during the CSAD events in 2015 and 2018 decreased
 289 by 34 μmol CO₂ m⁻² s⁻¹ and 26 μmol CO₂ m⁻² s⁻¹, respectively, compared to the respective long-term means of the reference
 290 periods (2005-2022; Figure 3b). During both CSAD years 2015 and 2018, cumulative GPP and Reco decreased
 291 considerably, although cumulative GPP tended to decrease more (>40 μmol CO₂ m⁻² s⁻¹) than Reco (>30 μmol CO₂ m⁻² s⁻¹;
 292 Figure 3d, f). In contrast, during the CSAD event in 2022, cumulative NEP decreased by 27 μmol CO₂ m⁻² s⁻¹ compared to
 293 long-term mean (Figure 3b), due to a decrease in cumulative GPP (by 44 μmol CO₂ m⁻² s⁻¹) and only negligible changes in
 294 Reco (Figure 3d, f). Furthermore, Rff fluxes during the 2018 and 2022 CSAD events were lower compared to the long-term
 295 mean of the reference period (2019-2021), with 23 μmol CO₂ m⁻² s⁻¹ and 32 μmol CO₂ m⁻² s⁻¹, respectively (Figure 3h). This
 296 decrease in Rff was supported by decreasing daily mean SR rates measured in 2022 (Figure 3g).

297 **Table 2. Daily mean CO₂ fluxes during CSAD events in 2015, 2018 and 2022 as well as their long-term means during the respective**
 298 **reference periods. Means and standard deviation (± SD) of net ecosystem production (NEP), partitioned gross primary productivity**
 299 **(GPP) and ecosystem respiration (Reco) as well as forest floor respiration (Rff) are given. The reference period for NEP, GPP and**
 300 **Reco represents all days between the 7th of July and the 23rd of August during 2005 and 2022; the reference period for Rff represents**
 301 **all days between the 14th of July and 23rd of August during 2019 and 2021. All fluxes are given in μmol CO₂ m⁻² s⁻¹. n.a. = not available.**

	NEP	GPP	Reco	Rff
CSAD 2015	2.09 ± 2.14	7.33 ± 2.54	5.05 ± 2.11	n.a.
CSAD 2018	1.99 ± 1.36	6.31 ± 1.44	4.23 ± 0.89	3.19 ± 0.68
CSAD 2022	1.89 ± 1.77	6.69 ± 1.33	5.73 ± 1.55	2.24 ± 0.20
Reference period	3.2 ± 0.82	8.77 ± 0.85	6.14 ± 0.65	3.81 ± 0.26



302

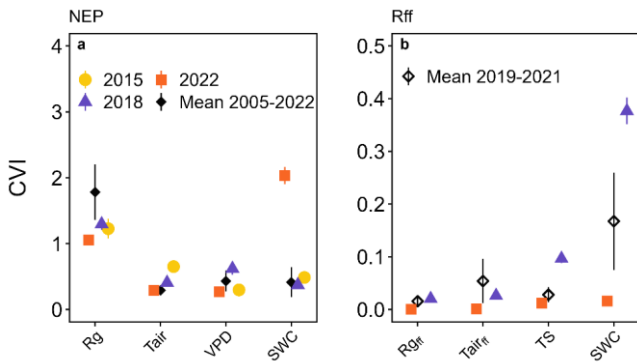
303 **Figure 3.** Comparison of daily mean (a) net ecosystem production (NEP), (bc) gross primary productivity (GPP), (eg) ecosystem
 304 respiration (Reco), and (dg) forest floor respiration (Rff) of the years when a CSAD event occurred (2015, 2018 and 2022) against
 305 the respective long-term means (a, c, e, g). The grey bands around the long-term means represent the standard error of the respective
 306 long-term mean CO₂ fluxes. Soil respiration (SR) measurements are given as daily means (\pm SD) measured manually in 2022 only.
 307 Thicker lines represent CSAD events. The right panels (b, d, f, h) show the cumulative difference between the actual fluxes recorded
 308 during a CSAD event and the respective long-term mean fluxes (2005-2022 for NEP, GPP and Reco; 2019-2021 for Rff-); the
 309 associated error bars show the cumulative standard errors of the long-term mean CO₂ fluxes for the respective CSAD event.

310 3.3 Drivers of NEP and Rff in 2015, 2018 and 2022

311 3.3.1 Comparison of drivers during the 2015, 2018, and 2022 with the long-term means

312 Daily mean NEP (NEP) during the growing seasons in 2015 and 2018; were mainly driven by daily mean incoming solar
 313 radiation (Rg), similar to the long-term daily mean NEP during 2005-2022 (Figure 4a). However, NEP during the 2022 growing
 314 season was more strongly driven by daily mean SWC than by Rg, as indicated by its high CVI (Figure 4a). Daily mean Tair
 315 and VPD were the second most important drivers of daily mean-NEP in 2015 and 2018, with a CVI higher than the ones for
 316 the long-term mean 2005-2022. DifferentlyIn contrast to NEP, daily mean Rff during the growing seasons 2019-2021 was

317 mainly driven by daily mean SWC, followed by daily mean T_{air} and daily-mean-TS (Figure 4b). We found that daily mean
 318 SWC was the main driver of daily-mean Rff in 2018, with a much higher CVI compared to those of other years, followed by
 319 daily mean TS. Overall, the CVI of all variables was much lower in 2022 compared to those of the other years (Figure 4b).



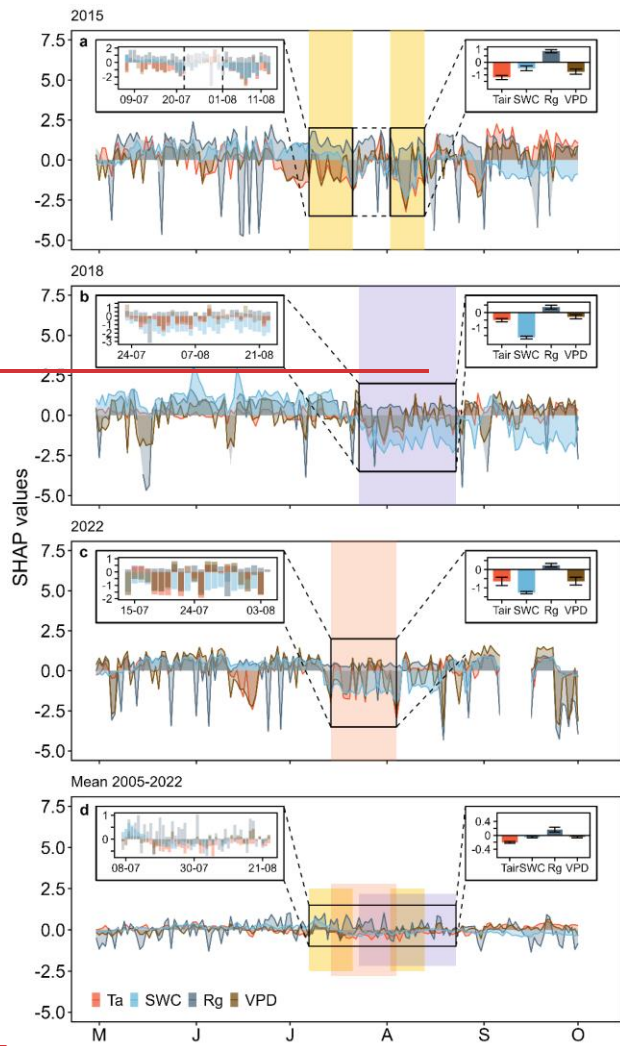
320
 321 **Figure 4. Driver analysis for daily mean (a) net ecosystem production (NEP) and (b) forest floor respiration (Rff) for the growing**
 322 **seasons 2015, 2018, 2022, compared with the long-term daily mean NEP 2005-2022 and the long-term daily mean Rff 2019-2021.**
 323 **calculated for each year separately. Note: Rff was not measured in 2015. The impaceteffect of driver (feature) variables is given by**
 324 **their conditional variable importance (CVI_h); Rg (incoming solar radiation), Tair (air temperature), VPD (vapor pressure deficit)**
 325 **and SWC (soil water content) were considered.**

326 3.3.2 Temporal development of important drivers of daytime NEP and daily Rff

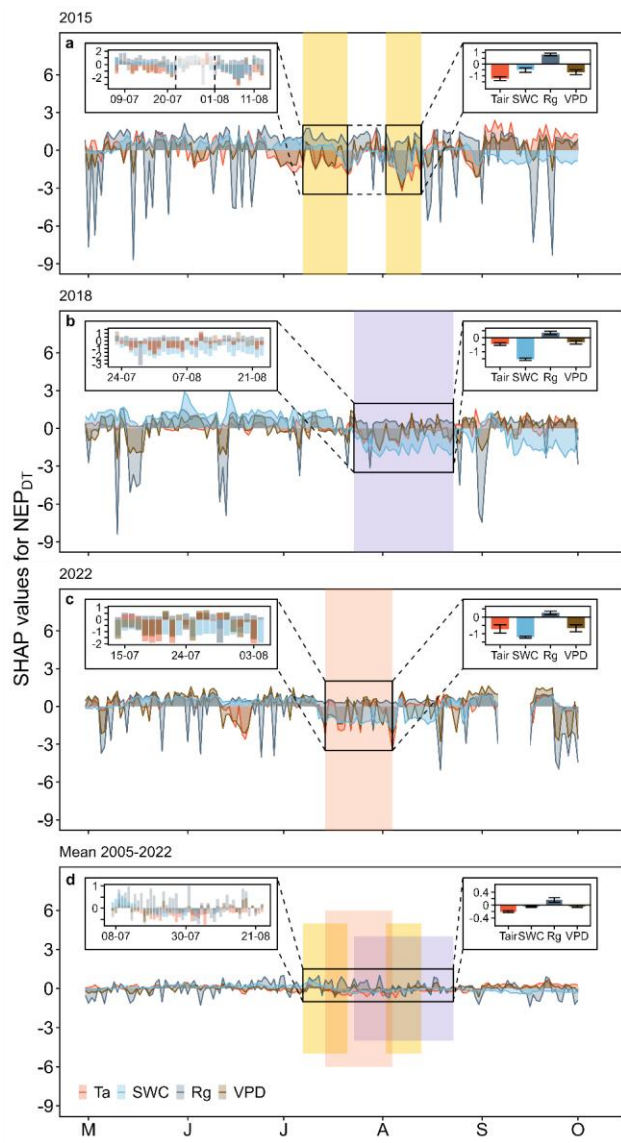
327 Testing the temporal development inof the main drivers efon daytime NEP with SHAP analysis revealed that overall, SWC,
 328 VPD and Tair decreased NEP during all CSAD events (Figure 5), while Rg increased daytime NEP. During the two CSAD
 329 events in 2015, both Tair and VPD were always associated with a decrease in NEP, while SWC exhibited a less consistent
 330 pattern, increasing NEP during the first CSAD event and decreasing NEP during the second (Figure 5a). Nevertheless, the
 331 mean contributions of Tair, SWC and VPD to daytime-mean-NEP Δ during the CSAD events of 2015 were negative, with
 332 Tair having the largest effect in reducing NEP (Figure 5a). As stated previously, Rg enhanced daytime-mean-NEP Δ in
 333 both CSAD events of 2015, contributing positively to NEP (Figure 5a). During the CSAD event of 2018, the mean
 334 contributions of Tair, VPD and SWC to daytime-mean-NEP Δ were also all negative, leading to a decrease in NEP (Figure
 335 5b). In contrast to 2015, SWC showed the largest negative effect on daytime NEP during the 2018 CSAD event, although it
 336 had clear positive effects prior to the CSAD onset. Rg both enhanced and decreased daytime-mean-NEP Δ during the
 337 CSAD event of 2018, which resulted in a small mean positive contribution (Figure 5b). As observed for 2018, the mean
 338 contributions of Tair, VPD and SWC were all negative during the CSAD event of 2022, leading to a decrease in NEP (Figure
 339 5c). Similarly to 2018, prior to the 2022 CSAD, SWC had a positive effect on daytime NEP, but then contributed the most to
 340 the decrease in NEP during the 2022 CSAD. As observed previously, Rg increased daytime NEP also during the 2022 CSAD

341 event, shown by its positive contribution (Figure 5c). Lastly, during the reference period 2005-2022 (from 7th of July to 23rd
342 of August), Tair, VPD and SWC affected daytime NEP negatively, although the contributions of VPD and SWC were close
343 to zero (Figure 5d). In contrast, the mean contribution of Rg to $\text{daytime-mean-NEP}_{\text{DT}}$ was positive, resulting in an increase
344 of $\text{daytime-mean-NEP}_{\text{DT}}$ during the reference period 2005-2022 (Figure 5d).

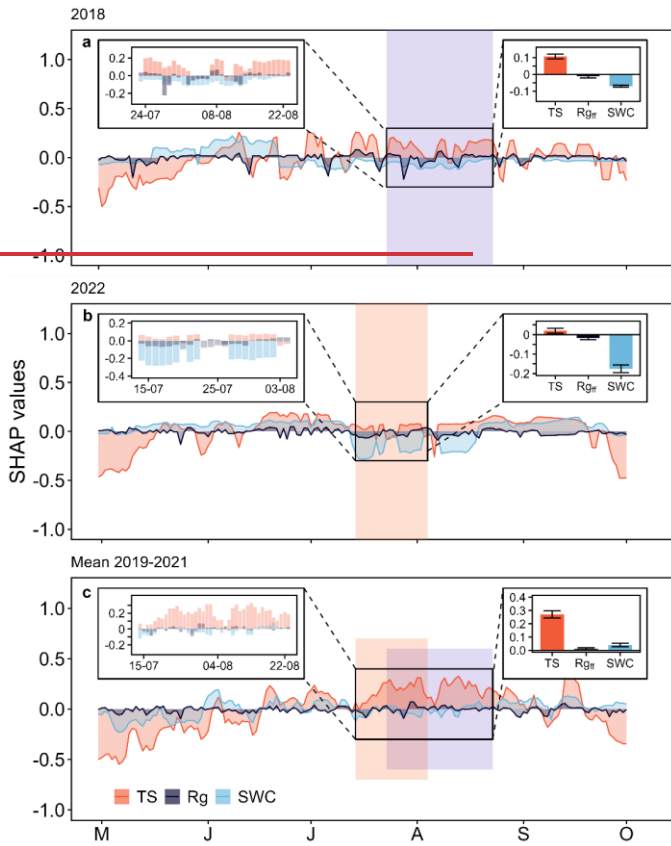
345 In accordance with the previous analysis for NEP, the decrease in daily Rff during both CSAD events of 2018 and 2022 was
346 mainly driven by negative effects of SWC (Figure 6a, b). In contrast, TS increased Rff during both CSAD events, but with
347 much larger effects during the CSAD in 2018 compared to that in 2022. This coincided with negative effects of SWC on Rff
348 already starting in mid-June, one month prior to the 2018 CSAD event (Figure 6a), while during the 2022 CSAD event, SWC
349 effects only became negative shortly before the 2022 event (Figure 6b). The effect of Rg_{ff} during both CSAD events in 2018
350 and 2022 was positive, but overall close to zero (Figure 6a, b). For comparison, during the reference period (from 14th of July
351 to 23rd of August 2019-2021), TS had the largest positive effect on Rff compared to the CSAD events in 2018 and 2022, which
352 persisted typically until September when senescence and leaf fall set in (Figure 6c). On the other hand, the effects of Rg_{ff} and
353 SWC varied around zero throughout all reference period summers (June, July, and August) (Figure 6c). Overall, mean
354 contributions to changes in Rff during the reference period 2019-2021 were dominated by positive effects by TS, and close to
355 zero contributions of Rg_{ff} and SWC (Figure 6c).



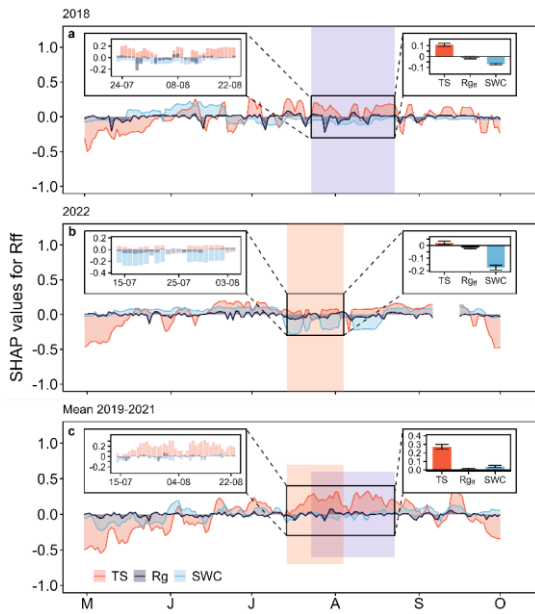
356



358 Figure 5. Temporal course of driverfeature contributions to daytime mean net ecosystem production (NEP) during the growing
 359 seasons of (a) 2015, (b) 2018, (c) 2022, and (d) the long-term mean (2005-2022), indicated by SHAP values for Tair, incoming
 360 radiation (Rg), VPD, and SWC. The small inserts on the left show the CSAD events (a-c) and the reference period for 2005-2022 (d).
 361 The small inserts on the right show mean (\pm SD) SHAP values for Tair, SWC, Rg and VPD during the CSAD events (a-c) and during
 362 the reference period for 2005-2022 (d). Positive SHAP values indicate positive effects on the response variable NEP, while negative
 363 SHAP values indicate negative effects. Coloured bands Coloured areas show the period in which a CSAD occurred in 2015, 2018 and
 364 2022 (a-c); they are also shown in panel (d) to highlight the reference period for the long-term mean (2005-2022).



365



366

367 **Figure 6. Temporal course of driver feature contributions to daily mean forest floor respiration (Rff) during the growing seasons of**
 368 **(a) 2018, (b) 2022, and (c) the non-CSAD years 2019-2021, indicated by SHAP values for soil temperature (TS), incoming radiation**
 369 **at the forest floor (Rgr), and SWC. The small inserts on the left show the CSAD events (a-b) and the reference period for 2019-2021**
 370 **(from 14th July to 23rd August) (d). The small inserts on the right show mean (\pm SD) SHAP values for TS, Rgr, and SWC during the**
 371 **CSAD events (a-b) and during the reference period for 2019-2021 (c). Positive SHAP values indicate a positive effect on the response**
 372 **variable Rff, while negative SHAP values indicate negative effects. Colour-bands/Coloured areas show the period in which a CSAD**
 373 **event occurred; they are also shown in panel (c) to highlight the reference period for 2019-2021.**

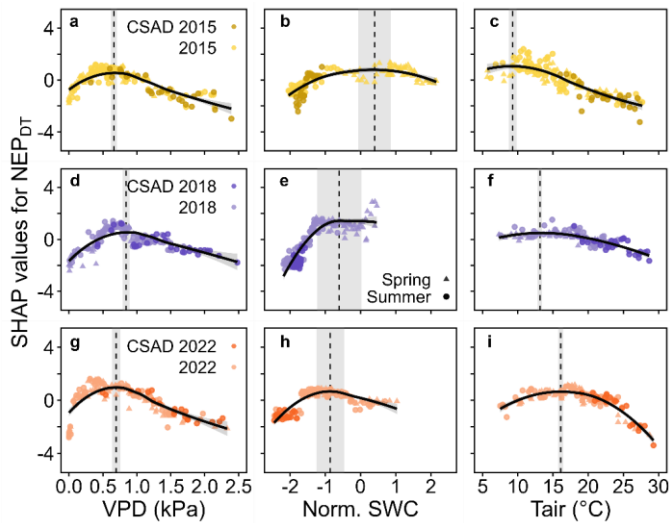
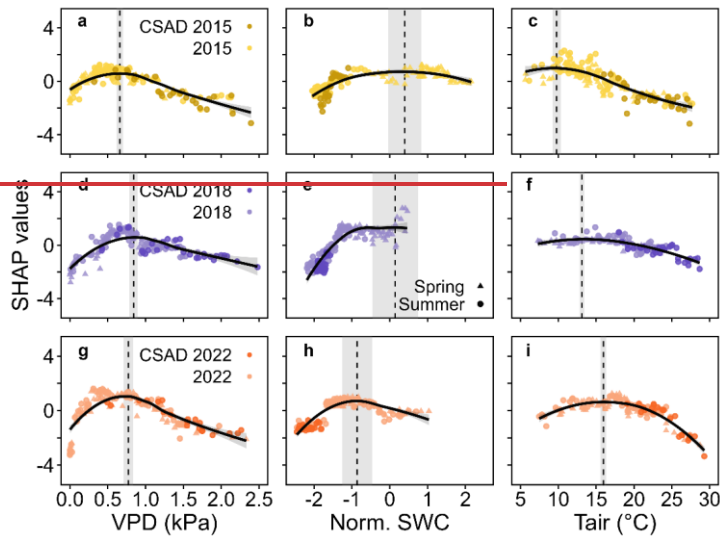
374 3.3.3 Driver thresholds with largest effects on daytime mean NEP and daily mean Rff for the CSAD years

375 We derived thresholds for the drivers VPD, SWC, Tair, and TS to understand if the absolute values of these drivers during
 376 the CSAD events actually differed from the absolute values that showed largest effects on daytime mean NEP or daily
 377 mean NEP_{DT} or Rff (based on the maximum marginal contributions from SHAP analysis). Threshold values differed among
 378 the CSAD years, particularly for SWC_{NEP_{max}} and SWC_{Rff_{max}} which were positive in 2015 and 2018 but negative in 2022
 379 (Table 3). VPD_{NEP_{max}} were relatively low for all CSAD years (between 0.7 and 0.8 kPa), while Tair_{NEP_{max}} increased
 380 from around 10 °C in 2015 to 13 °C in 2018 to 16 °C in 2022. For comparison, TS_{Rff_{max}} were around 19 °C in 2018 and 15.6
 381 °C in 2022. Comparing measured driver values to those thresholds revealed that most daytime mean VPD values during the
 382 CSAD events were typically higher than the respective VPD_{NEP_{max}} threshold for each of the CSAD years, reaching values
 383 of up to 2.5 kPa (Figure 7a, d, g), only few exceptions occurred. In contrast, all daytime mean SWC values measured during

384 the CSAD events were far below the SWC_NEP_{max} thresholds in all CSAD years (Figure 7b, e, h), resulting in very negative
385 effects on daytime NEP. We also observed a decrease in SWC_NEP_{max} values from 2015 to 2022 (Figure 7b, e, h; Table 3).
386 Likewise, daytime mean Tair measured during the CSAD events was far above the Tair_NEP_{max} threshold for all CSAD events
387 (Figure 7c, f, i; Table 3). In addition, we observed an increase in Tair_NEP_{max} values from 2015 to 2022 (Figure 7c, f, i; Table
388 3). We also observed positive relationships between SWC_NEP_{max} and mean SWC as well as between VPD_NEP_{max} and mean
389 VPD over the different growing seasons (Figure A5). Applying the same analysis to daily mean Rff (Figure 8) revealed that
390 daily mean TS measured during the CSAD event in 2018 varied around the TS_Rff_{max} threshold of 2018 (Figure 8a), while
391 measured TS values were higher than the TS_Rff_{max} threshold during the CSAD event in 2022 (Figure 8b). As observed for
392 the NEP, SWC values measured during the CSAD events of 2018 and 2022 were far below the respective SWC_Rff_{max}
393 thresholds (Figure 8b, d), with measured data as well as SWC_Rff_{max} thresholds being much lower in 2022 than in 2018 (Figure
394 8b, d; Table 3).

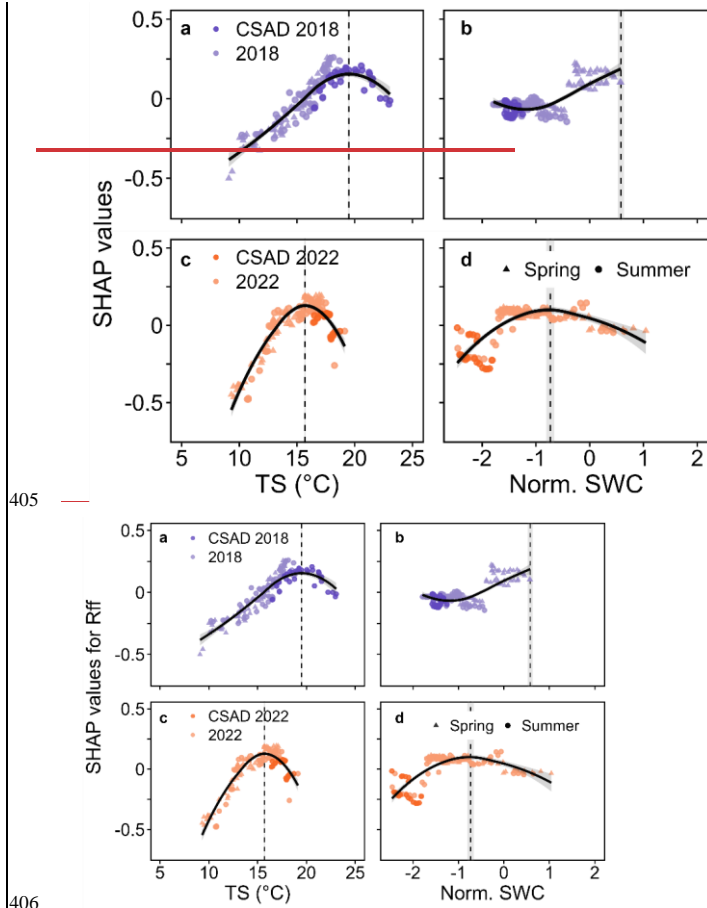
395 **Table 3. Absolute driver thresholds (mean ± SE) related to the most positivelargest effect on NEPNEP_{Dr} or Rff during the three**
396 **CSAD years and the long-term means (2005-2022 for NEP and 2019-2021 for Rff). Identification was based on the maximum**
397 **marginal contribution of the respective driver (VPD, SWC, Tair and TS) in the SHAP analysis for each year.**

Year	VPD_NEP _{max} (kPa)	SWC_NEP _{max} (normalised)	Tair_NEP _{max} (°C)	TS_Rff _{max} (°C)	SWC_Rff _{max} (normalised)
2015	0.66 ± 0.04	0.40 ± 0.43	9.79 ± 0.56	n.a.	n.a.
2018	0.84 ± 0.05	0.14 ± 0.6	13.13 ± 0.30	19.15 ± 0.07	0.58 ± 0.07
2022	0.77 ± 0.06	-0.86 ± 0.4	15.95 ± 0.37	15.60 ± 0.07	- 0.73 ± 0.09



398
399
400 **Figure 7. Detection of VPD, SWC and Tair values corresponding to the maximum rate of daytime mean net ecosystem production**
401 **(NEP_{DT}) during the growing seasons of 2015, 2018 and 2022. Positive or negative SHAP values represent positive or negative**

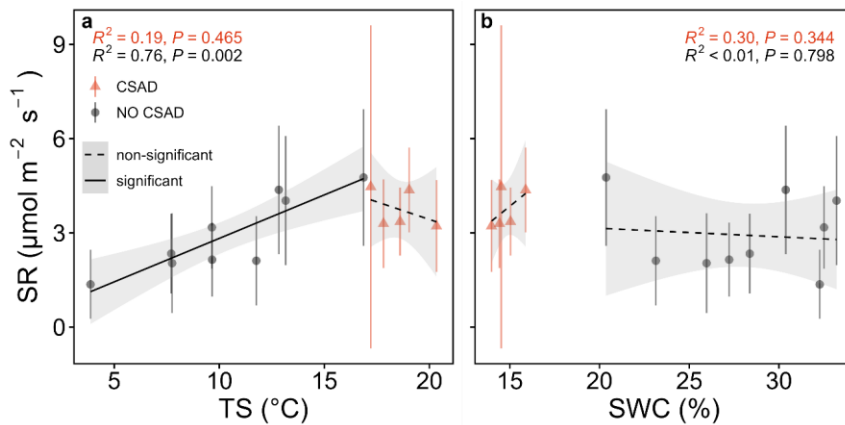
402 effects on $NEP_{NEP_{gr}}$. The vertical dashed lines and the grey ribbons bands show VPD (a, d, g), SWC (b, e, h), and Tair (c, f, i) and
 403 their standard deviations, corresponding to the most positive largest effect on $NEP_{NEP_{gr}}$ based on the respective maximum marginal
 404 contribution of the respective driver in the SHAP analysis for each year to NEP for 2015, 2018 and 2022.



407 Figure 8. Detection of soil temperature (TS) and SWC values corresponding to the maximum rate of daily mean forest floor
 408 respiration (Rff) in 2018 and 2022. Positive or negative SHAP values represent positive or negative effects on Rff. The vertical dashed
 409 lines and grey ribbons bands show TS (a, c) and SWC (b, d) and their standard deviations, corresponding to the most positive largest
 410 effect on Rff based on the respective maximum marginal contribution of the respective driver in the SHAP analysis for each year to
 411 Rff in 2018 and 2022.

412 3.4 SR responses to TS and SWC in 2022

413 As seen above, daily mean SR rates mirrored the responses of Rff (Figure 3), though with a much coarser time resolution. The
414 relationships of SR with TS and SWC varied, depending if CSAD events were considered or not (Figure 9). When no CSAD
415 event was recorded, daily mean SR significantly increased with TS ($R^2 = 0.76$, P of 0.002; linear regression). However,
416 during the CSAD event, ~~daily mean SR tended to decrease with increasing TS~~ ($R^2 = 0.19$; Figure 9a). On the
417 other hand, ~~when no independent if a CSAD event was recorded, daily mean or not~~, SR did not respond to variation in SWC
418 ($R^2 < 0.01$), while ~~daily mean SR tended to increase with SWC during the CSAD event~~ (R^2 of 0.30 and $R^2 = 0.3$ respectively; Figure
419 9b).



420
421 **Figure 9. Linear relationships of daily mean soil respiration (SR) with (a) soil temperature (TS) and (b) soil water content (SWC)**
422 **during the CSAD event 2022 and the rest of the year 2022. Two models were fitted separately for the periods with and without the**
423 **CSAD event. The goodness of the fit is expressed with R^2 and p-values (P) in the respective panels according to the colour scale.**

424 4 Discussion

425 In this study, we identified three compound soil and atmospheric drought (CSAD) events during the last 18 years (i.e., 2015,
426 2018, and 2022) for a mountain mixed deciduous forest. Although they were of comparable intensity, they differed in terms
427 of their timing. We further assessed the mainly negative impacts of these CSAD events on ecosystem CO_2 fluxes (NEP, GPP,
428 Reco) and forest floor respiration (Rff). Moreover, we quantified the temporal contribution of the main drivers to these fluxes
429 during the CSAD events and the respective growing seasons (VPD, Tair, Rg, SWC, TS). Pronounced differences in driver
430 ~~impacts/effects~~ as well as their temporal development were found; for ecosystem vs. forest floor fluxes, but also among drivers
431 and among CSAD events. In addition, we saw first signs of acclimation ~~of NEP~~ to such CSAD events, ~~making i.e., changed~~

432 sensitivities of NEP to its drivers, both within the same and among different growing seasons. This also suggested that
433 predictions of site-specific CSADs and their impacts might become more challenging in the future.

434 4.1 Compound soil and atmospheric drought (CSAD) events

435 Several recent studies have shown that Europe already did and also will experience an increase in intensity and frequency of
436 CSAD conditions in the future (e.g., Shekhar et al., 2023; Markonis et al., 2021). Such increased occurrence of extremes was
437 also evident during the 18 years (2005-2022) of eddy-covariance measurements at CH-Lae, with three years (2015, 2018,
438 2022) being characterized by CSAD events, all within the last eight years (2015-2022). Two other years, 2019 and 2020, also
439 characterized by atmospheric drought, albeit at lower intensity than the three years ~~chosen~~identified here (Figure 1), did not
440 show co-occurring soil drought at our forest site, and were therefore not ~~identified~~classified as CSAD years. This nicely
441 illustrated site-specific environmental conditions playing a relevant role when discussing the impact of extreme compound
442 events at larger spatial scales (Shekhar et al., 2023). Interestingly, even though the intensities of the CSAD events of 2015,
443 2018 and 2022 were comparable in terms of SWC and VPD values, the pre-conditions and the time of occurrence were
444 different. Pre-conditions (late-spring or early summer), especially in terms of soil moisture and temperature or VPD, can be
445 wet and cool, near-normal, or dry and warm. Thus, depending on these pre-conditions, the impact of any CSAD event on forest
446 performance will differ as shown here. Prior to a CSAD event, soil moisture plays a vital role in determining how well the
447 forest can resist and also recover from the stress of a CSAD event (Jiao et al., 2021). Dry and warm vs. non-limiting conditions
448 before the CSAD event can put the forest under additional water stress during the CSAD event, making it more susceptible to
449 drought and heat stress (da Costa et al., 2018). However, even prior normal soil moisture and warm conditions in spring which
450 favour productivity, but are also accompanied by increased water demands for evapotranspiration, lead to increased soil dryin g,
451 and can thus amplify extreme dryness stress during summer drought as observed during the 2018 CSAD event at our mixed
452 deciduous forest site (CH-Lae) and across Central Europe (Gharun et al., 2020; Bastos et al., 2020; Shekhar et al., 2020). Thus,
453 CSAD events will require our full attention in the future, since their impacts will strongly differ not only depending on their
454 frequency, duration, and intensity, but also depending on the prior site-specific environmental conditions the ecosystem
455 experiences.

456 4.2 Forest CO₂ fluxes and their respective drivers

457 4.2.1 Net Ecosystem Productivity, NEP

458 The CSAD events of 2015, 2018 and 2022 resulted in a significant decrease in NEP, which was largely due to decreasing GPP*
459 (between ~~4516~~ and ~~3028~~%), while ecosystem respiration (Reco) either decreased or did not change compared to the long-term
460 mean at the mixed deciduous forest. Such reductions in GPP during CSAD events have been observed in earlier studies,
461 particularly for beech, the dominant species at our forest site (Ciais et al. 2005; Bastos et al., 2020; Dannenberg et al., 2022;
462 D'Orangeville et al., 2018; Xu et al., 2020; Gharun et al., 2020). Increased stomatal closure in response to high VPD and low

Formatted: Space After: 12 pt

463 soil moisture (i.e., stomatal response), reduction of photosynthesis due to reduced carboxylation rate (Rubisco activity) at high
464 temperatures (i.e., non-stomatal response; Buckley, 2019; Gourlez de la Motte et al., 2020) at leaf level as well as reduced
465 canopy conductance at ecosystem level (Ciais et al. 2003, Granier et al. 2007, Gharun et al. 2020) are typically associated with
466 such CSAD events.

467 Our driver analysis revealed that, ~~among the considered features,~~ air temperature ~~did not have an important impact~~ had the
468 ~~largest effect~~ on reducing NEP_{DT} during ~~all three~~ the CSAD ~~events,~~ event in 2015, but not in the others suggesting that
469 stomatal responses on GPP were ~~generally~~ more relevant than temperature-related non-stomatal responses (Granier et al.,
470 2007). Moreover, the major drivers we identified, i.e., VPD and SWC, support stomatal responses as underlying mechanisms
471 for the reduction of net CO₂ uptake via GPP (Dannenberget al., 2022; Fu et al., 2022; [Petek-Petrik et al., 2023](#); van der Woude
472 et al., 2023) during all ~~three~~ CSAD events in 2015, 2018, and 2022. However, the contributions of those dryness-related
473 variables varied among the CSAD events, suggesting that the response of the forest differed depending on the respective
474 intensity of soil dryness (SWC) and of air dryness (VPD) during the CSAD events. Also, the conditions prior to the CSAD
475 event seemed to play an important role, as SWC was more important for NEP during the 2022 CSAD event, which followed
476 upon a prevailing soil drought, compared to the 2015 and 2018 CSAD events.

477 Another line of argumentation towards dryness-related vs. temperature-related drivers of reduced NEP during CSAD events
478 is related to Reco with its two major components, i.e., plant and soil respiration. In our study, Reco was between ~~6-30-7-31~~%
479 lower during the three CSAD ~~events~~ years compared to the other years, supporting the dryness- over the temperature-related
480 argumentation. While plant respiration typically increases in response to high temperatures (Schulze et al. 2019), it also
481 depends on the intensity of the event: if substrate (i.e., carbohydrate) availability is diminished during a CSAD event due to
482 reduced GPP, respiration can also decrease (Janssens et al. 2001; Ciais et al., 2005; Von Buttlar et al., 2018), albeit typically
483 less than GPP (Schwalm et al. 2010). Similarly, soil respiration decreases when substrate supply for root and microbial
484 respiration is low (Högberg et al. 2001; RUEHR et al. 2009). Moreover, soil respiration is known to be small when soil moisture
485 is low (due to reduced microbial and root respiration) during CSAD events (-Ruehr et al. 2010; Von Buttlar et al., 2018; Wang
486 et al., 2014), as seen at our site in 2022.

487 In addition to the standard response of NEP (and its components GPP and Reco) to abiotic ~~factors~~ drivers (VPD, SWC and
488 Tair), NEP sensitivity to ~~abiotic factors~~ those drivers could change from one growing season to another, ([Grossman, 2023](#)),
489 especially during drought conditions, indicating ~~drought~~-acclimation of NEP (Crous et al., 2022; Aspinwall et al., 2017;
490 Sendall et al., 2015; Sperlich et al., 2019). This difference in NEP sensitivity to VPD, SWC and Tair during ~~the~~ 2015, 2018,
491 and 2022 growing ~~season~~ seasons was clearly observed in our study (see response curves in Figure 7). The thresholds derived
492 from the response curves of SHAP values vs. the abiotic ~~factors~~ drivers (Figure 7) indicated ~~drought~~-acclimation of NEP to
493 higher VPD (in 2018 and 2022), and lower SWC (in 2022), ~~as we observed a shift towards drier conditions of the VPD, and~~
494 ~~SWC values corresponding to the maximum marginal contribution of the features to NEP_{DT} in CSAD years (Figure 7, A5).~~

Formatted: Space After: 12 pt

495 Such drought acclimations could be due to biophysical adjustments such as access of soil water from deeper soil layers
496 (Brinkmann et al., 2019), changes in photosynthetic thermal acclimation and changes in stomatal sensitivity to VPD (Aspinwall
497 et al., 2017; Smith and Dukes, 2017; Gessler et al., 2020). Such NEP acclimation to higher VPD and lower SWC will be critical
498 in the future, enabling forests to persist (longer) during CSAD events (Kumarathunge et al., 2019).

499 4.2.2 Forest floor and soil respiration, R_{ff} and SR

500 The CSAD event in 2022 resulted in a more pronounced and rapid decrease of R_{ff} than in 2018, leading to smaller CO₂ losses
501 from the forest floor compared to 2018 CSAD and the reference period 2019-2021. We observed a similar seasonal trend of
502 R_{ff} and SR, but SR was consistently higher than R_{ff} (Figure 3d). R_{ff} is indeed composed by soil and understory vegetation
503 respiration. At the CH-Lae site, the understory LAI (Leaf Area Index) decreased in late spring (Paul-Limoges, 2017) when
504 trees leaf-out, and light reaching the forest floor diminishes. Thus, during the growing season, most of the respiratory CO₂
505 fluxes from below the canopy consist of SR. Yet, a small part of the SR can be offset by photosynthesis of the vegetation still
506 growing below the canopy (i.e., seedlings of *Fagus sylvatica* and other herbaceous plants). As we observed that GPP_{ff} was not
507 different from zero during the growing seasons (Figure A4, appendix-AA6), we here assumed the effect of photosynthesis in
508 the daily R_{ff} being negligible. European mixed forests are usually more resistant to drought than monospecific ones in terms
509 of microbial soil respiration (Gillespie et al., 2020). For example, Gillespie et al. (2020) found that CO₂ emissions were not
510 decreasing under drought in natural mixed European forests. However, a reduction of SR during drought has been
511 widely reported in other studies (e.g., Ruehr et al., 2010; Schindlbacher et al., 2012; Wang et al., 2014; Sun et al., 2019), but
512 the interplay of intensity, duration, and biotic components can trigger different responses of the forest floor in the respective
513 ecosystems (Talmon et al., 2011; Jiao et al., 2021).

514 The decreased importance of TS during the CSAD event of 2018 and 2022 compared to the reference period 2019-2021 (Figure
515 6) was driven by the limitation of R_{ff} and SR by SWC. In accordance with the SR analysis, we found no effect of TS during
516 the CSAD event in 2022 (Figure 9). Drought periods in forests can indeed diminish the temperature sensitivity of the SR
517 (Jassal et al., 2008; Ruehr et al. 2010; Sun et al., 2019; Schindlbacher et al., 2012; van Straaten et al., 2011; Wang et al., 2014).
518 Generally, SWC is not limiting at the CH-Lae site, but exceptions can occur during summer (Knohl et al., 2008; Ruehr
519 et al., 2010; Trabucco and Zomer, 2022). We know that SR is the sum of heterotrophic and autotrophic respiration (Ruehr and
520 Buchmann, 2009; Wang et al., 2014; Zheng et al., 2021). A large component of heterotrophic respiration is microbial activity
521 in the soil. Under drought, the microbial activity is typically reduced by the limited diffusion of soluble carbon substrate for
522 extracellular enzymes (Manzoni et al., 2012). Consequently, litter decomposition rates also decrease (Deng et al., 2021). If
523 decomposition rates decrease, soil organic matter increases in the soil, resulting in higher C and N in the soil (van der Molen
524 et al., 2011). At the same time, drought reduces photosynthesis and so plants tend to keep non-structural carbohydrates in the
525 leaves or roots to sustain the living tissues (Högberg et al., 2008). Thereby, root activity and production are downregulated

Formatted: Subscript

526 (Deng et al., 2021), which can lead to a decoupling of photosynthetic and underground activities (Ruehr et al., 2009; Barba et
527 al., 2018). Eventually, soil drought can significantly alter the N and C cycle in the ecosystem (Deng et al., 2021).

528 The TS and SWC at which $R_{ff,max}$ was observed varied from growing season to growing season, as we saw for 2018 and 2022
529 (Figure 8). The SWC recorded during the CSAD events was clearly below ~~than the~~ $SWC_{R_{ff,max}}$, but the TS recorded during
530 the CSAD events was observed to be in the range of $TS_{R_{ff,max}}$ in 2018. The interplay and the seasonal trends of TS and SWC
531 can thus determine at which abiotic conditions the highest respiration rate is found. Even though SR is projected to increase
532 under global warming (Schindlbacher et al., 2012), the more frequent occurrence of droughts (Grillakis, 2019) could partially
533 offset those emissions (Zheng et al., 2021), as we observed in the decrease of Rff during CSAD events. However, the decrease
534 in CO₂ emissions can be compensated by CO₂ bursts from rain events occurring after drought periods (Lee et al., 2002) as we
535 observed ~~in~~ after the CSAD event in 2022 (Figure 3d). In general, a recovery of SR is expected if ~~the~~ soil moisture quickly
536 returns to normal conditions (Yao et al., 2023). Yet, biotic factors like fine roots are crucial for ~~tree~~ recovery after drought
537 (Netzer et al., 2016; Hikino et al., 2021; Hikino et al., 2022). For example, it is well known that the fine roots of *Fagus sylvatica*
538 can grow to deeper soil depths during drought, but only if the drought is not too severe, ~~then~~ when they can be shed
539 (Hildebrandt, et al., 2020). Indeed, Nickel et al., (2017) found a progressive decrease in vital fine roots after repeated drought
540 in a mixed deciduous forest in Europe. Hence, the pre-and post-conditions, the timing, the intensity, and the duration of a
541 CSAD are very important to predict the consequences in terms of respiratory CO₂ emissions (~~Wang et al., 2014~~).

542 5 Conclusions

543 ~~In this study~~ For our mixed deciduous forest, we found first signs of forest's-NEP ~~to acclimate~~ acclimation to more extreme soil
544 (low SWC) and atmospheric drought (high VPD) conditions ~~when comparing sensitivities of NEP to these drivers during the~~
545 ~~same growing season~~, which will be fundamental for drought resistance in the future. Nevertheless, we expect to witness a
546 larger reduction of GPP with more extreme CSAD events in the future, even if complemented by a reduction in Reco. Hence
547 responses to CSAD events might lead to a reduction of the CO₂ sink capacity of the forest in the future. The study also
548 highlighted ~~a decoupling between the drivers and the different behaviours of the~~ responses of ~~the above-canopy and the~~ forest
549 floor CO₂ fluxes during CSAD events. With further global warming in Europe, we expect an increase in Rff, but with more
550 extreme droughts and more intense precipitation events, we assume a higher variability of the CO₂ emissions from forest soils
551 and thus uncertain consequences for the respective soil carbon stocks. Ultimately, the consequences of ~~such~~ CSAD events will
552 influence the annual carbon budget of a forest, and thus jeopardising many restoration/reforestation projects or nature-based
553 solutions as proposed in the Paris Agreement.

554 **Appendix A**

555 **Table A1. List of instruments, models and manufacturers used in this study.**

Instrument	Model	Manufacturer
Infrared gas analyser (IRGA) ¹	LI-7500 (2004-2015)	LI-COR Inc., Lincoln, NE, USA
Infrared gas analyser (IRGA) ¹	LI-7200 (2016-2022)	LI-COR Inc., Lincoln, NE, USA
3-D Sonic anemometer ¹	HS-50	Gill Instruments Ltd., Lymington, UK
Air temperature and relative humidity ²	Rotronic MP 101 A	Rotronic AG, Bassersdorf, Switzerland
Incoming radiation ²	BF2_BF2116	Delta-T Devices Ltd, Cambridge, UK
Infrared gas analyser (IRGA) ³	LI-7500	LI-COR Inc., Lincoln, NE, USA
3-D Sonic anemometer ³	R-350	Gill Instruments Ltd., Lymington, UK
Air temperature and relative humidity ⁴	CS215_E16511	Campbell Scientific Ltd., UG, USA
Soil temperature and water content ⁵	Decagon ECH2O EC-20 probes (2004-2020)	Pullman, WA, USA
Soil temperature and water content ⁵	TEROS 12_00007171 (2020-2022)	METER Group AG, NE, USA
Incoming radiation ⁴	LI190SB-L	LI-COR Inc., Lincoln, NE, USA
Infrared gas analyser (IRGA) ⁶	LI-8100	LI-COR Inc., Lincoln, NE, USA
Soil temperature ⁶	GTH 175 PT	GHM Messtechnik GmbH, Regenstauf, Germany
Soil water content ⁶	HH2 Moisture Meter	Delta-T Devices, Cambridge, United Kingdom

¹Above-canopy EC system (47 m height)

²Above-canopy meteorological measurements (54 m height)

³Below-canopy EC system (1.5 m height)

⁴Below-canopy meteorological station (2 m height)

⁵Forest floor meteorological station (profile measurements up to at 5, 10, 20, 30, 50 cm depth)

⁶Portable sensors (SR survey measurements)

Formatted: Line spacing: single

Formatted: Line spacing: single

Formatted: Line spacing: single

Formatted: Line spacing: single

Formatted: Line spacing: single

Formatted: Line spacing: single

Formatted: Line spacing: single

Formatted: Line spacing: single

Formatted: Line spacing: single

Formatted: Line spacing: single

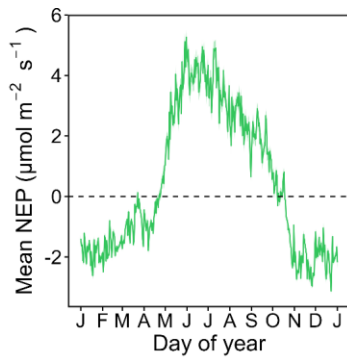
Formatted: Line spacing: single

Formatted: Line spacing: single

Formatted: Line spacing: single

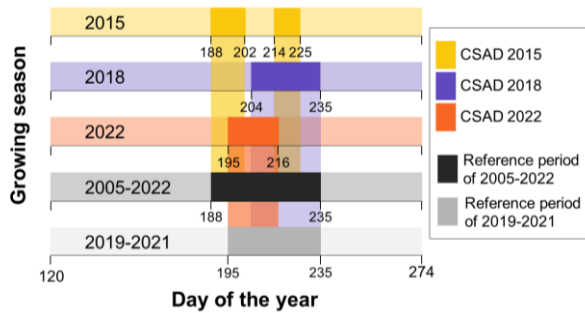
Formatted: Line spacing: single

Formatted: Font color: Auto



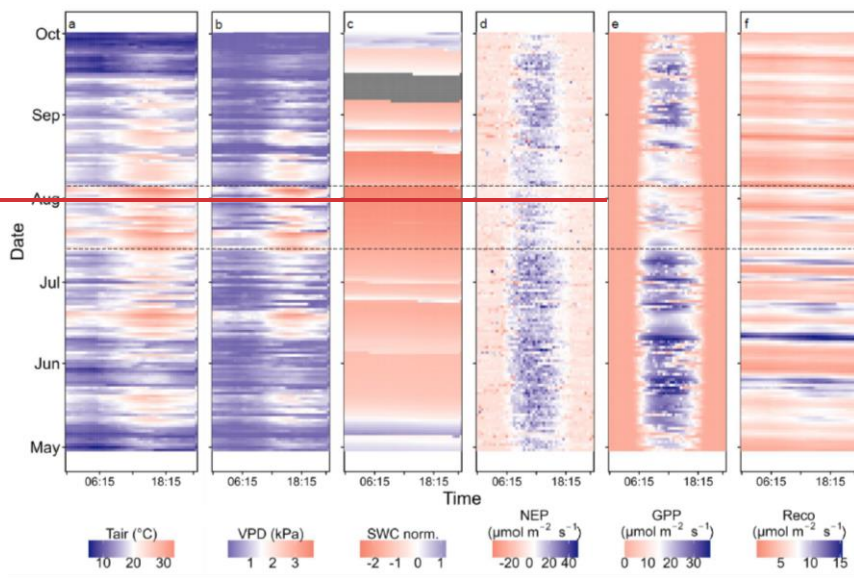
556

557 Figure A1. Long-term (2005-2022) daily mean and standard deviation of net ecosystem productivity (NEP) of CH-Lae. The zero-
 558 line highlights whether the daily NEP is positive or negative. The growing season (GS) was identified as the period in which daily
 559 NEP was positive (1st May to 31st September).

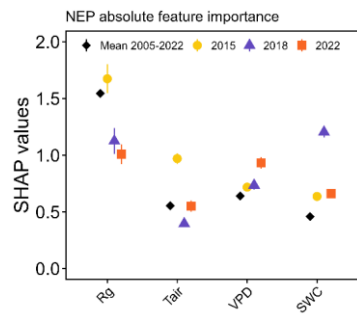


560

561 Figure A2. Graphical definition of reference periods. The five horizontal beads bars display the three growing seasons in which a
 562 CSAD event occurred, and the two long term means used as reference periods for comparison period (2005-2022 for ecosystem
 563 level measurements and 2019-2021 for forest floor measurements). The CSAD periods are marked for each growing season in the
 564 CSAD years. The reference period of the mean 2005-2022 used in the analysis corresponds to the interval of time
 565 between day 188 (7th July) and day 235 (23rd of August), while the one of the mean 2019-2021 corresponds to the interval of time
 566 between day 195 (14th July) and day 235 (23rd of August).
 567

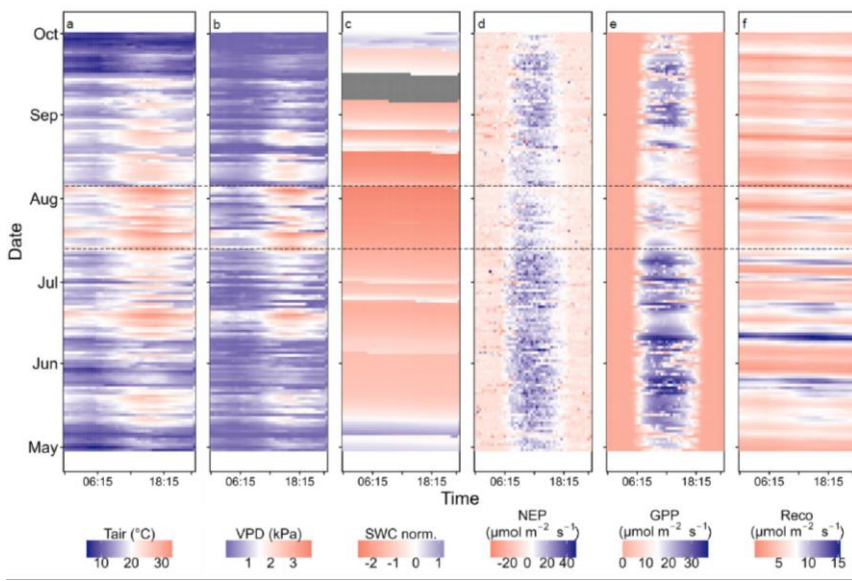


568



569

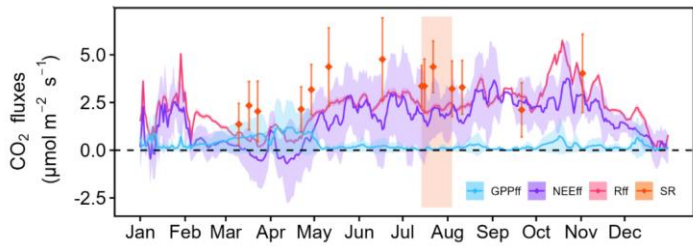
570 **Figure A3.** Absolute mean SHAP values (\pm SE) for daily mean NEP obtained with the XGBoost model.



571

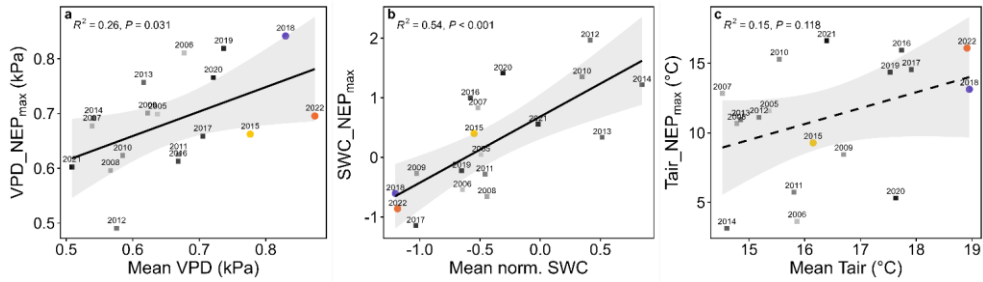
572 **Figure A4.** Diurnal (x-axis) and intra-annual (y-axis) variation of (a) air temperature (Tair), (b) VPD, (c) normalized soil water
 573 content (SWC at 20 cm depth) (d) net ecosystem production (NEP), (e) gross primary productivity (GPP), and (f) ecosystem
 574 respiration (Reco) in during the 2022 growing season. 30 min averages are plotted in all panels. The two black dashed lines extending
 575 fromat 14th July 2022 toand 4th August 2022 mark the compound soil and atmospheric drought (CSAD) event of summer 2022.

Formatted: Superscript
 Formatted: Superscript

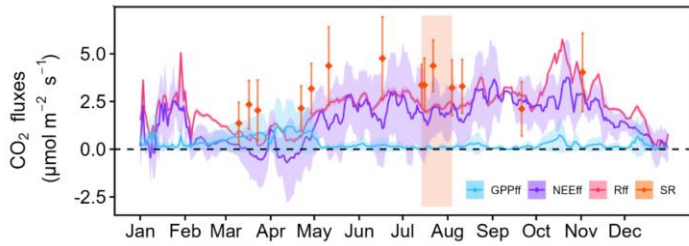


576

577 Figure A4.



578
579 **Figure A5.** Linear regressions of mean VPD, SWC, and Tair values during the growing season of a given year against maximum
580 marginal contributions of VPD, SWC and Tair (here abbreviated as feature NEP_{max}) to daytime NEP. SWC values were normalized.
581 The grey bands around the regression lines indicate the 95% confidence interval. R² and p-values are given as well.



582
583 **Figure A6.** Forest floor CO₂ fluxes in 2022. The continuous lines show gap-filled and partitioned daily mean fluxes and standard
584 deviations (coloured ribbons) of the forest floor bands. 30 min averages are plotted. The diamonds represent daily means of manual
585 soil respiration measurements, standard deviations are given as well. The area colored in orange band represents the CSAD event
586 of 2022.

587 Code availability

588 The R scripts used for the data analysis and plots are available.
589 The R scripts used for data analyses and plots are available in the Git repository with the following link
590 <https://github.com/lscapucci/Compound-soil-and-atmospheric-drought-events-and-CO2-fluxes-of-a-mixed-deciduous-forest>.

591 **Author contribution**

592 LS, AS, MG, NB conceptualization of the study, LS, AS, SAB, AB field campaigns, LS, AS, LH data processing and
593 management, LS, AS data analyses ~~and; LS, AS, NB~~ manuscript writing, ~~and all the~~ authors revision and editing of the
594 manuscript.

595 **Competing interests**

596 The contact author has declared that none of the authors has any competing interests.

597 **Acknowledgements**

598 Authors acknowledge funding from the ETH Zürich project FEVER (ETH-27 19-1), and the SNF funded projects COCO
599 (200021_197357), ICOS-CH Phase 3 (20F120_198227), and EcoDrive (IZCOZ0_198094), and the great support of the
600 Grassland Sciences group members, especially Anna Katarina Gilgen, Luana Krebs, Julia Hauri, Franziska Richter, Yi Wang,
601 Fabio Turco, Ruikun Gou, Roland Anton Werner, and Davide Andreatta.

602 **References**

- 603 Anderegg, W. R. L., Wu, C., Acil, N., Carvalhais, N., Pugh, T. A. M., Sadler, J. P., and Seidl, R.: A climate risk analysis of
604 Earth's forests in the 21st century, *Science*, 377, 1099-1103, 10.1126/science.abp 9723, 2022.
- 605 Aspinwall, M. J., Vårhammar, A., Blackman, C. J., Tjoelker, M. G., Ahrens, C., Byrne, M., Tissue, D. T., and Rymer, P. D.:
606 Adaptation and acclimation both influence photosynthetic and respiratory temperature responses in, *Tree Physiology*, 37,
607 1095-1112, 10.1093/treephys/tpx047, 2017.
- 608 Aubinet, M., Vesala, T., and Papale, D.: Eddy covariance: a practical guide to measurement and data analysis, Springer Science
609 & Business Media 2012.
- 610 Barba, J., Lloret, F., Poyatos, R., Molowny-Horas, R., and Yuste, J. C.: Multi-temporal influence of vegetation on soil
611 respiration in a drought-affected forest, *Iforest-Biogeosciences and Forestry*, 11, 189-198, 10.3832/ifor2448-011, 2018.
- 612 Bastos, A., Ciaias, P., Friedlingstein, P., Sitch, S., Pongratz, J., Fan, L., Wigneron, J. P., Weber, U., Reichstein, M., Fu, Z.,
613 Anthoni, P., Arneth, A., Haverd, V., Jain, A. K., Joetjzer, E., Knauer, J., Lienert, S., Loughran, T., McGuire, P. C., Tian,
614 H., Viovy, N., and Zaehle, S.: Direct and seasonal legacy effects of the 2018 heat wave and drought on European ecosystem
615 productivity, *Science Advances*, 6, [ARTN eaba2724](https://doi.org/10.1126/sciadv.aba2724), 10.1126/sciadv.aba2724, 2020.
- 616 ~~Bates, D., Mächler, M., Bolker, B. M., and Walker, S. C.: Fitting Linear Mixed Effects Models Using lme4, *Journal of*~~
617 ~~Statistical Software~~, 67, 1-48, DOI-10.18637/jss.v067.i01, 2015.

Formatted: Indent: Left: 0 cm, Hanging: 0.5 cm

618 Birami, B., Gattmann, M., Heyer, A. G., Grote, R., Arneth, A., and Ruehr, N. K.: Heat Waves Alter Carbon Allocation and
619 Increase Mortality of Aleppo Pine Under Dry Conditions, *Frontiers in Forests and Global Change*, 1, [ARTN 8](#),
620 10.3389/ffgc.2018.00008, 2018.

621 Bogati, K. and Walczak, M.: The Impact of Drought Stress on Soil Microbial Community, Enzyme Activities and Plants,
622 *Agronomy-Basel*, 12, [ARTN 189](#), 10.3390/agronomy12010189, 2022.

623 Breiman, L.: Random forests, *Machine Learning*, 45, 5-32, Doi 10.1023/A:1010933404324, 2001.

624 Brinkmann, N., Eugster, W., Buchmann, N., and Kahmen, A.: Species-specific differences in water uptake depth of mature
625 temperate trees vary with water availability in the soil, *Plant Biology*, 21, 71-81, 10.1111/plb.12907, 2019.

626 Buckley, T. N.: How do stomata respond to water status?, *New Phytologist*, 224, 21-36, 10.1111/nph.15899, 2019.

627 Chen, T. and Guestrin, C.: XGBoost: A Scalable Tree Boosting System, *Proceedings of the 22nd ACM SIGKDD International
628 Conference on Knowledge Discovery and Data Mining, San Francisco, California, USA*, 10.1145/2939672.2939785, 2016.

629 Chi, J. S., Zhao, P., Klosterhalfen, A., Jocher, G., Kljun, N., Nilsson, M. B., and Peichl, M.: Forest floor fluxes drive differences
630 in the carbon balance of contrasting boreal forest stands, *Agricultural and Forest Meteorology*, 306, [ARTN 108454](#),
631 10.1016/j.agrformet.2021.108454, 2021.

632 Ciaia, P., Reichstein, M., Viovy, N., Granier, A., Ogée, J., Allard, V., Aubinet, M., Buchmann, N., Bernhofer, C., Carrara, A.,
633 Chevallier, F., De Noblet, N., Friend, A. D., Friedlingstein, P., Grünwald, T., Heinesch, B., Keronen, P., Knohl, A., Krinner,
634 G., Loustau, D., Manca, G., Matteucci, G., Miglietta, F., Ourcival, J. M., Papale, D., Pilegaard, K., Rambal, S., Seufert, G.,
635 Soussana, J. F., Sanz, M. J., Schulze, E. D., Vesala, T., and Valentini, R.: Europe-wide reduction in primary productivity
636 caused by the heat and drought in 2003, *Nature*, 437, 529-533, 10.1038/nature03972, 2005.

637 Copernicus Climate Change Service: European State of the Climate 2019, ~~2019~~ <https://climate.copernicus.eu/ESOTC/2019>,
638 [2019](#).

639 Copernicus Climate Change Service (C3S): European State of the Climate 2022,
640 <https://climate.copernicus.eu/esotc/2022>, [2023](#).

641 Crous, K. Y., Uddling, J., and De Kauwe, M. G.: Temperature responses of photosynthesis and respiration in evergreen trees
642 from boreal to tropical latitudes, *New Phytologist*, 234, 353-374, 10.1111/nph.17951, 2022.

643 da Costa, A. C. L., Rowland, L., Oliveira, R. S., Oliveira, A. A. R., Binks, O. J., Salmon, Y., Vasconcelos, S. S., Junior, J. A.
644 S., Ferreira, L. V., Poyatos, R., Mencuccini, M., and Meir, P.: Stand dynamics modulate water cycling and mortality risk
645 in droughted tropical forest, *Global Change Biology*, 24, 249-258, 10.1111/gcb.13851, 2018.

646 Dannenberg, M. P., Yan, D., Barnes, M. L., Smith, W. K., Johnston, M. R., Scott, R. L., Biederman, J. A., Knowles, J. F.,
647 Wang, X., Duman, T., Litvak, M. E., Kimball, J. S., Williams, A. P., and Zhang, Y.: Exceptional heat and atmospheric
648 dryness amplified losses of primary production during the 2020 U.S. Southwest hot drought, *Glob Chang Biol*, 28, 4794-
649 4806, 10.1111/gcb.16214, 2022.

650 de la Motte, L. G., Beauclair, Q., Heinesch, B., Cuntz, M., Foltynová, L., Sigut, L., Kowalska, N., Manca, G., Ballarin, I. G.,
651 Vincke, C., Roland, M., Ibrom, A., Lousteau, D., Siebicke, L., Neiryink, J., and Longdoz, B.: Non-stomatal processes

Formatted: Indent: Left: 0 cm, Hanging: 0.5 cm

652 reduce gross primary productivity in temperate forest ecosystems during severe edaphic drought, *Philosophical*
653 *Transactions of the Royal Society B-Biological Sciences*, 375, [ARTN 20190527](#), 10.1098/rstb.2019.0527, 2020.

654 Deng, L., Peng, C. H., Kim, D. G., Li, J. W., Liu, Y. L., Hai, X. Y., Liu, Q. Y., Huang, C. B., Shanguan, Z. P., and Kuzyakov,
655 Y.: Drought effects on soil carbon and nitrogen dynamics in global natural ecosystems, *Earth-Science Reviews*, 214, [ARTN](#)
656 [10350](#), 10.1016/j.earscirev.2020.103501, 2021.

657 Dirmeyer, P. A., Balsamo, G., Blyth, E. M., Morrison, R., and Cooper, H. M.: Land-~~Atmosphere Interactions Exacerbated-~~
658 ~~atmosphere interactions exacerbated~~ the ~~Droughtdrought~~ and ~~Heatwave Over Northernheatwave over northern~~ Europe
659 ~~During Summerduring summer~~ 2018, *AguaAGU Advances*, 2, [ARTN e2020AV000283](#), 10.1029/2020AV000283, 2021.

660 D'Orangeville, L., Maxwell, J., Kneeshaw, D., Pederson, N., Duchesne, L., Logan, T., Houle, D., Arseneault, D., Beier, C. M.,
661 Bishop, D. A., Druckenbrod, D., Fraver, S., Girard, F., Halman, J., Hansen, C., Hart, J. L., Hartmann, H., Kaye, M.,
662 Leblanc, D., Manzoni, S., Ouimet, R., Rayback, S., Rollinson, C. R., and Phillips, R. P.: Drought timing and local climate
663 determine the sensitivity of eastern temperate forests to drought, *Global Change Biology*, 24, 2339-2351,
664 10.1111/gcb.14096, 2018.

665 ~~Etzold, S., Buchmann, N., and Eugster, W.: Contribution of advection to the carbon budget measured by eddy covariance at a~~
666 ~~steep mountain slope forest in Switzerland, *Biogeosciences*, 7, 2461-2475, 10.5194/bg-7-2461-2010, 2010.~~

667 ~~Etzold, S., Ruehr, N. K., Zweifel, R., Dobbertin, M., Zingg, A., Pluess, P., Häslér, R., Eugster, W., and Buchmann, N.: The~~
668 ~~Carbon Balance of Two Contrasting Mountain Forest Ecosystems in Switzerland: Similar Annual Trends, but Seasonal~~
669 ~~Differences, *Ecosystems*, 14, 1289-1309, 10.1007/s10021-011-9481-3, 2011.~~

670 Fan, S. M., Wofsy, S. C., Bakwin, P. S., Jacob, D. J., and Fitzjarrald, D. R.: Atmosphere-~~Biosphere Exchangebiosphere*~~
671 ~~exchange~~ of ~~Co2CO₂~~ and ~~O₃~~ in the Central-Amazon-Forest, *Journal of Geophysical Research-Atmospheres*, 95, 16851-
672 16864, DOI 10.1029/JD095iD10p16851, 1990.

673 Foken, T., Göckede, M., Mauder, M., Mahrt, L., Amiro, B., and Munger, W.: Post-field data quality control, in: *Handbook*
674 *of micrometeorology: a guide for surface flux measurement and analysis*, Springer, 181-208, 2004.

675 Fratini, G., Ibrom, A., Arriga, N., Burba, G., and Papale, D.: Relative humidity effects on water vapour fluxes measured with
676 closed-path eddy-covariance systems with short sampling lines (~~vol 165, pg 53, 2012~~), *Agricultural and Forest*
677 *Meteorology*, 166, 234-234, 10.1016/j.agrformet.2012.10.013, 2012.

678 Gazol, A. and Camarero, J. J.: Compound climate events increase tree drought mortality across European forests, *Science of*
679 *the Total Environment*, 816, [ARTN 151604](#), 10.1016/j.scitotenv.2021.151604, 2022.

680 George, J. P., Bürkner, P. C., Sanders, T. G. M., Neumann, M., Cammalleri, C., Vogt, J. V., and Lang, M.: Long-term forest
681 monitoring reveals constant mortality rise in European forests, *Plant Biology*, 24, 1108-1119, 10.1111/plb.13469, 2022.

682 Gessler, A., Bottero, A., Marshall, J., and Arend, M.: The way back: recovery of trees from drought and its implication for
683 acclimation, *New Phytologist*, 228, 1704-1709, 10.1111/nph.16703, 2020.

684 Gharun, M., Hörtnagl, L., Paul-Limoges, E., Ghiasi, S., Feigenwinter, I., Burri, S., Marquardt, K., Etzold, S., Zweifel, R.,
685 Eugster, W., and Buchmann, N.: Physiological response of Swiss ecosystems to 2018 drought across plant types and

Formatted: Indent: Left: 0 cm, Hanging: 0.5 cm

Formatted: Subscript

686 elevation, Philosophical Transactions of the Royal Society B-Biological Sciences, 375, [ARTN 20190521](#),
687 10.1098/rstb.2019.0521, 2020.

688 Gillespie, L. M., Fromin, N., Milcu, A., Buatois, B., Pontoizeau, C., and Hättenschwiler, S.: Higher tree diversity increases
689 soil microbial resistance to drought, Communications *Biology*, 3, [ARTN 377](#), [10.1038/s42003-020-1112-0](#), 2020.
690 [10.1038/s42003-020-1112-0](#), 2020.

691 ~~Gillespie, L. M., Fromin, N., Milcu, A., Buatois, B., Pontoizeau, C., and Hättenschwiler, S.: Higher tree diversity increases
692 soil microbial resistance to drought, Communications Biology, 3, ARTN 377
693 10.1038/s42003-020-1112-0, 2020.~~

694 [Greco, S. and Baldocchi, D. D.: Seasonal variations of CO₂ and water vapour exchange rates over a temperate deciduous forest,
695 *Global Change Biology*, 2, 183-197, \[10.1111/j.1365-2486.1996.tb00071.x\]\(#\), 1996.](#)

696 Grillakis, M. G.: Increase in severe and extreme soil moisture droughts for Europe under climate change, Science of ~~the~~
697 Total Environment, 660, 1245-1255, [10.1016/j.scitotenv.2019.01.001](#), 2019.

698 Grossiord, C., Buckley, T. N., Cernusak, L. A., Novick, K. A., Poulter, B., Siegwolf, R. T. W., Sperry, J. S., and McDowell,
699 N. G.: Plant responses to rising vapor pressure deficit, New Phytologist, 226, 1550-1566, [10.1111/nph.16485](#), 2020.

700 Grossiord, C., Sevanto, S., Borrego, I., Chan, A. M., Collins, A. D., Dickman, L. T., Hudson, P. J., McBranch, N., Michaletz,
701 S. T., Pockman, W. T., Ryan, M., Vilagrosa, A., and McDowell, N. G.: Tree water dynamics in a drying and warming
702 world, Plant Cell and Environment, 40, 1861-1873, [10.1111/pce.12991](#), 2017.

703 [Grossman, J. J.: Phenological physiology: seasonal patterns of plant stress tolerance in a changing climate, New Phytologist,
704 237, 1508-1524, 2023.](#)

705 Haberstroh, S., Werner, C., Grün, M., Kreuzwieser, J., Seifert, T., Schindler, D., and Christen, A.: Central European 2018 hot
706 drought shifts scots pine forest to its tipping point, Plant Biology, 24, 1186-1197, [10.1111/plb.13455](#), 2022.

707 Harris, N. L., Gibbs, D. A., Baccini, A., Birdsey, R. A., de Bruin, S., Farina, M., Fatoyinbo, L., Hansen, M. C., Herold, M.,
708 Houghton, R. A., Potapov, P. V., Suarez, D. R., Roman-Cuesta, R. M., Saatchi, S. S., Slay, C. M., Turubanova, S. A., and
709 Tyukavina, A.: Global maps of twenty-first century forest carbon fluxes, Nature Climate Change, 11, [10.1038/s41558-020-
710 00976-6](#), 2021.

711 Hermann, M., Röthlisberger, M., Gessler, A., Rigling, A., Senf, C., Wohlgemuth, T., and Wernli, H.: Meteorological history
712 of low-forest-greenness events in Europe in 2002-2022, Biogeosciences, 20, 1155-1180, [10.5194/bg-20-1155-2023](#), 2023.

713 Hikino, K., Danzberger, J., Riedel, V. P., Rehschuh, R., Ruehr, N. K., Hesse, B. D., Lehmann, M. M., Buegger, F., Weigl, F.,
714 Pritsch, K., and Grams, T. E. E.: High resilience of carbon transport in long-term drought-stressed mature Norway spruce
715 trees within 2 weeks after drought release, Global Change Biology, 28, 2095-2110, [10.1111/gcb.16051](#), 2022.

716 Hikino, K., Danzberger, J., Riedel, V. P., Hesse, B. D., Hafner, B. D., Gebhardt, T., Rehschuh, R., Ruehr, N. K., Brunn, M.,
717 Bauerle, T. L., Landhäusser, S. M., Lehmann, M. M., Rötzer, T., Pretzsch, H., Buegger, F., Weigl, F., Pritsch, K., and
718 Grams, T. E. E.: Dynamics of initial carbon allocation after drought release in mature Norway spruce-Increased

Formatted: Indent: Left: 0 cm, Hanging: 0.5 cm

Formatted: Indent: Left: 0 cm, Hanging: 0.5 cm

719 belowground allocation of current photoassimilates covers only half of the carbon used for fine-root growth, *Global Change*
720 *Biology*, 28, 6889-6905, 10.1111/gcb.16388, 2022.

721 Hildebrandt, A.: ~~Root-Water-Relations~~water relations and ~~Interactions~~interactions in ~~Mixed-Forest-Settings~~mixed forest
722 settings, *Forest-Water Interactions*, 240, 319-348, 10.1007/978-3-030-26086-6_14, 2020.

723 Högberg, P., Nordgren, A., Buchmann, N., Taylor, A. F. S., Ekblad, A., Högberg, M. N., Nyberg, G., Ottosson-Löfvenius, M.,
724 and Read, D. J.: Large-scale forest girdling shows that current photosynthesis drives soil respiration, *Nature*, 411, 789-792,
725 Doi 10.1038/35081058, 2001.

726 Högberg, P., Högberg, M. N., Göttlicher, S. G., Betson, N. R., Keel, S. G., Metcalfe, D. B., Campbell, C., Schindlbacher, A.,
727 Hurry, V., Lundmark, T., Linder, S., and Näsholm, T.: High temporal resolution tracing of photosynthate carbon from the
728 tree canopy to forest soil microorganisms, *New Phytologist*, 177, 220-228, 10.1111/j.1469-8137.2007.02238.x, 2008.

729 Horst, T. W.: A simple formula for attenuation of eddy fluxes measured with first-order-response scalar sensors, *Boundary-*
730 *Layer Meteorology*, 82, 219-233, Doi 10.1023/A:1000229130034, 1997.

731 Hothorn, T., Hornik, K., and Zeileis, A.: Unbiased recursive partitioning: A conditional inference framework, *Journal of*
732 *Computational and Graphical Statistics*, 15, 651-674, 10.1198/106186006x133933, 2006.

733 Intergovernmental Panel on Climate, C.: *Climate Change 2022 – Impacts, Adaptation and Vulnerability: Working Group II*
734 *Contribution to the Sixth Assessment Report of the Intergovernmental Panel on Climate Change*, Cambridge University
735 Press, Cambridge, ~~DOI~~-10.1017/9781009325844, 2023.

736 Ionita, M., Dima, M., Nagavciuc, V., Scholz, P., and Lohmann, G.: Past megadroughts in central Europe were longer, more
737 severe and less warm than modern droughts, *Communications Earth & Environment*, 2, ~~ARTN-61~~
738 10.1038/s43247-021-00130-w, 2021.

739 Ionita, M., Tallaksen, L. M., Kingston, D. G., Stagge, J. H., Laaha, G., Van Lanen, H. A. J., Scholz, P., Chelcea, S. M., and
740 Haslinger, K.: The European 2015 drought from a climatological perspective, *Hydrology and Earth System Sciences*, 21,
741 1397-1419, 10.5194/hess-21-1397-2017, 2017.

742 Janssens, I. A., Lankreijer, H., Matteucci, G., Kowalski, A. S., Buchmann, N., Epron, D., Pilegaard, K., Kutsch, W., Longdoz,
743 B., Grünwald, T., Montagnani, L., Dore, S., Rebmann, C., Moors, E. J., Grelle, A., Rannik, Ü., Morgenstern, K., Oltchev,
744 S., Clement, R., Gudmundsson, J., Minerbi, S., Berbigier, P., Ibrom, A., Moncrieff, J., Aubinet, M., Bernhofer, C., Jensen,
745 N. O., Vesala, T., Granier, A., Schulze, E. D., Lindroth, A., Dolman, A. J., Jarvis, P. G., Ceulemans, R., and Valentini, R.:
746 Productivity overshadows temperature in determining soil and ecosystem respiration across European forests, *Global*
747 *Change Biology*, 7, 269-278, ~~DOI~~-10.1046/j.1365-2486.2001.00412.x, 2001.

748 Jassal, R. S., Black, T. A., Novak, M. D., Gaumont-Guay, D., and Nesic, Z.: Effect of soil water stress on soil respiration and
749 its temperature sensitivity in an 18-year-old temperate Douglas-fir stand, *Global Change Biology*, 14, 1305-1318,
750 10.1111/j.1365-2486.2008.01573.x, 2008.

Formatted: Indent: Left: 0 cm, Hanging: 0.5 cm

751 Jiao, T., Williams, C. A., De Kauwe, M. G., Schwalm, C. R., and Medlyn, B. E.: Patterns of post-drought recovery are strongly
752 influenced by drought duration, frequency, post-drought wetness, and bioclimatic setting, *Global Change Biology*, 27,
753 4630-4643, 10.1111/gcb.15788, 2021.

754 Kim, J. B., So, J. M., and Bae, D. H.: Global Warming ~~Impacts~~ [impacts](#) on ~~Severe Drought Characteristics~~ [severe drought](#)
755 [characteristics](#) in Asia ~~Monsoon Region~~ [monsoon region](#), *Water*, 12, ~~ARTN-1360~~
756 10.3390/w12051360, 2020.

757 Kittler, F., Eugster, W., Foken, T., Heimann, M., Kolle, O., and Göckede, M.: High-quality eddy-covariance CO_2
758 CO_2 budgets under cold climate conditions, *Journal of Geophysical Research-Biogeosciences*, 122, 2064-2084,
759 10.1002/2017jg003830, 2017.

760 Knohl, A., Soe, A. R. B., Kutsch, W. L., Göckede, M., and Buchmann, N.: Representative estimates of soil and ecosystem
761 respiration in an old beech forest, *Plant and Soil*, 302, 189-202, 10.1007/s11104-007-9467-2, 2008.

762 Körner, C., Möhl, P., and Hiltbrunner, E.: Four ways to define the growing season, *Ecology Letters*, 10.1111/ele.14260, 2023.

763 Kumarathunge, D. P., Medlyn, B. E., Drake, J. E., Tjoelker, M. G., Aspinwall, M. J., Battaglia, M., Cano, F. J., Carter, K. R.,
764 Cavaleri, M. A., Cernusak, L. A., Chambers, J. Q., Crous, K. Y., De Kauwe, M. G., Dillaway, D. N., Dreyer, E., Ellsworth,
765 D. S., Ghannoum, O., Han, Q. M., Hikosaka, K., Jensen, A. M., Kelly, J. W. G., Kruger, E. L., Mercado, L. M., Onoda,
766 Y., Reich, P. B., Rogers, A., Slot, M., Smith, N. G., Tarvainen, L., Tissue, D. T., Togashi, H. F., Tribuzy, E. S., Uddling,
767 J., Vårhammar, A., Wallin, G., Warren, J. M., and Way, D. A.: Acclimation and adaptation components of the temperature
768 dependence of plant photosynthesis at the global scale, *New Phytologist*, 222, 768-784, 10.1111/nph.15668, 2019.

769 Lal, P., Shekhar, A., Gharun, M., and Das, N. N.: Spatiotemporal evolution of global long-term patterns of soil moisture,
770 *Science of the Total Environment*, 867, ~~ARTN-161470~~, 10.1016/j.scitotenv.2023.161470, 2023.

771 Lasslop, G., Reichstein, M., Papale, D., Richardson, A. D., Armeth, A., Barr, A., Stoy, P., and Wohlfahrt, G.: Separation of net
772 ecosystem exchange into assimilation and respiration using a light response curve approach: critical issues and global
773 evaluation, *Global Change Biology*, 16, 187-208, 10.1111/j.1365-2486.2009.02041.x, 2010.

774 Lee, M.-S., Nakane, K., Nakatsubo, T., Mo, W.-H., and Koizumi, H.: Effects of rainfall events on soil CO_2 flux in a
775 cool temperate deciduous broad-leaved forest, *Ecological Research*, 17, 401-409, ~~UNSP-ere_498.sem~~ [10.1046/j.1440-](#)
776 [1703.2002.00498.x, 2002.](#)
777 ~~DOI-10.1046/j.1440-1703.2002.00498.x, 2002.~~

778 Lloyd, J. and Taylor, J. A.: On the ~~Temperature Dependence~~ [temperature-dependence](#) of ~~Soil Respiration~~ [soil respiration](#),
779 *Functional Ecology*, 8, 315-323, ~~Doi~~ 10.2307/2389824, 1994.

780 Lu, R. Y., Xu, K., Chen, R. D., Chen, W., Li, F., and Lv, C. Y.: Heat waves in summer 2022 and increasing concern regarding
781 heat waves in general, *Atmospheric and Oceanic Science Letters*, 16, ~~ARTN-100290~~, 10.1016/j.aosl.2022.100290, 2023.

782 Lundberg, S. M. and Lee, S. I.: A Unified Approach to ~~Interpreting Model Predictions~~, [Advances interpreting model](#)
783 [predictions, advances](#) in ~~Neural Information Processing Systems 30 (Nips 2017)~~, [neural information processing systems](#),
784 30, 2017.

Formatted: Indent: Left: 0 cm, Hanging: 0.5 cm

Formatted: Indent: Left: 0 cm, Hanging: 0.5 cm

Formatted: Indent: Left: 0 cm, Hanging: 0.5 cm

785 Lundberg, S. M., Erion, G., Chen, H., DeGrave, A., Prutkin, J. M., Nair, B., Katz, R., Himmelfarb, J., Bansal, N., and Lee, S.
786 I.: From local explanations to global understanding with explainable AI for trees, *Nature Machine Intelligence*, 2, 56-67,
787 10.1038/s42256-019-0138-9, 2020.

788 Manzoni, S., Schimel, J. P., and Porporato, A.: Responses of soil microbial communities to water stress: results from a meta-
789 analysis, *Ecology*, 93, 930-938, Doi 10.1890/11-0026.1, 2012.

790 Markonis, Y., Kumar, R., Hanel, M., Rakovec, O., Máca, P., and AghaKouchak, A.: The rise of compound warm-season
791 droughts in Europe, *Science Advances*, 7, ~~ARTN eabb9668~~, 10.1126/sciadv.abb9668, 2021.

792 Martinez-Garcia, E., Nilsson, M. B., Laudon, H., Lundmark, T., Fransson, J. E. S., Wallerman, J., and Peichl, M.: Overstory
793 dynamics regulate the spatial variability in forest-floor CO₂ fluxes across a managed boreal forest landscape, *Agricultural*
794 *and Forest Meteorology*, 318, ~~ARTN 108916~~, 10.1016/j.agrformet.2022.108916, 2022.

795 ~~Mauder, M. and Foken, T.: Impact of post-field data processing on eddy covariance flux estimates and energy balance closure.~~
796 ~~Meteorologische Zeitschrift, 15, 597-610, 2006.~~

797 MeteoSvizzera. (2023). Rapporto sul clima 2022.

798 Miralles, D. G., Gentile, P., Seneviratne, S. I., and Teuling, A. J.: Land-atmospheric feedbacks during droughts and heatwaves:
799 state of the science and current challenges, *Annals of the New York Academy of Sciences*, 1436, 19-35,
800 10.1111/nyas.13912, 2019.

801 Moncrieff, J., Clement, R., Finnigan, J., and Meyers, T.: Averaging, detrending, and filtering of eddy covariance time series,
802 in: *Handbook of micrometeorology: A guide for surface flux measurement and analysis*, Springer, 7-31, 2004.

803 Moravec, V., Markonis, Y., Rakovec, O., Svoboda, M., Trnka, M., Kumar, R., and Hanel, M.: Europe under multi-year
804 droughts: how severe was the 2014-2018 drought period?, *Environmental Research Letters*, 16, ~~ARTN~~
805 ~~0340624010~~, 1088/1748-9326/abe828, 2021.

806 Netzer, F., Thöm, C., Celepirovic, N., Ivankovic, M., Alfarraj, S., Dounavi, A., Simon, J., Herschbach, C., and Rennenberg,
807 H.: Drought effects on C, N, and P nutrition and the antioxidative system of beech seedlings depend on geographic origin,
808 *Journal of Plant Nutrition and Soil Science*, 179, 136-150, 10.1002/jpln.201500461, 2016.

809 Nickel, U. T., Weikl, F., Kerner, R., Schäfer, C., Kallenbach, C., Munch, J. C., and Pritsch, K.: Quantitative losses vs.
810 qualitative stability of ectomycorrhizal community responses to 3 years of experimental summer drought in a beech-spruce
811 forest, *Global Change Biology*, 24, E560-E576, 10.1111/gcb.13957, 2018.

812 Obladen, N., Dechering, P., Skiadasis, G., Tegel, W., Kessler, J., Höllerl, S., Kaps, S., Hertel, M., Dulamsuren, C., Seifert,
813 T., Hirsch, M., and Seim, A.: Tree mortality of European beech and Norway spruce induced by 2018-2019 hot droughts in
814 central Germany, *Agricultural and Forest Meteorology*, 307, ~~ARTN 10.1016/j.agrformet.2021.108482~~, 2021.
815 ~~10.1016/j.agrformet.2021.108482~~, 2021.

816 Orth, R.: When the ~~Land Surface Shifts Gears~~, ~~Aguland surface shifts gears~~, *AGU Advances*, 2, ~~ARTN e2021AV000414~~,
817 10.1029/2021AV000414, 2021.

Formatted: Subscript

Formatted: Indent: Left: 0 cm, Hanging: 0.5 cm

Formatted: Indent: Left: 0.5 cm

818 Paul-Limoges, E., Wolf, S., Eugster, W., Hörtnagl, L., and Buchmann, N.: Below-canopy contributions to ecosystem CO₂
819 fluxes in a temperate mixed forest in Switzerland, *Agricultural and Forest Meteorology*, 247, 582-596,
820 10.1016/j.agrformet.2017.08.011, 2017.

821 Paul-Limoges, E., Wolf, S., Schneider, F. D., Longo, M., Moorcroft, P., Gharun, M., and Damm, A.: Partitioning
822 evapotranspiration with concurrent eddy covariance measurements in a mixed forest, *Agricultural and Forest*
823 *Meteorology*, 280, [ARTN-10778610](#)10.1016/j.agrformet.2019.107786, 2020.

824 Pei, F. S., Li, X., Liu, X. P., and Lao, C. H.: Assessing the impacts of droughts on net primary productivity in China, *Journal*
825 *of Environmental Management*, 114, 362-371, 10.1016/j.jenvman.2012.10.031, 2013.

826 [Petek-Petrik, A., Húdoková, H., Fleischer, P., Jamnická, G., Kurjak, D., Sliacka Konôpková, A., and Petrik, P.: The](#)
827 [combined effect of branch position, temperature, and VPD on gas exchange and water-use efficiency of Norway spruce,](#)
828 [Biologia plantarum, 67, 136, 2023.](#)

829 Reichstein, M., Falge, E., Baldocchi, D., Papale, D., Aubinet, M., Berbigier, P., Bernhofer, C., Buchmann, N., Gilmanov, T.,
830 Granier, A., Grünwald, T., Havránková, K., Ilvesniemi, H., Janous, D., Knohl, A., Laurila, T., Lohila, A., Loustau, D.,
831 Matteucci, G., Meyers, T., Miglietta, F., Ourcival, J. M., Pumpanen, J., Rambal, S., Rotenberg, E., Sanz, M., Tenhunen,
832 J., Seufert, G., Vaccari, F., Vesala, T., Yakir, D., and Valentini, R.: On the separation of net ecosystem exchange into
833 assimilation and ecosystem respiration: review and improved algorithm, *Global Change Biology*, 11, 1424-1439,
834 10.1111/j.1365-2486.2005.001002.x, 2005.

835 Ruehr, N. K. and Buchmann, N.: Soil respiration fluxes in a temperate mixed forest: seasonality and temperature sensitivities
836 differ among microbial and root-rhizosphere respiration, *Tree Physiology*, 30, 165-176, 10.1093/treephys/tpp106, 2010.

837 Ruehr, N. K., Knohl, A., and Buchmann, N.: Environmental variables controlling soil respiration on diurnal, seasonal and
838 annual time-scales in a mixed mountain forest in Switzerland, *Biogeochemistry*, 98, 153-170, 10.1007/s10533-009-9383-
839 z, 2010.

840 Ruehr, N. K., Offermann, C. A., Gessler, A., Winkler, J. B., Ferrio, J. P., Buchmann, N., and Barnard, R. L.: Drought effects
841 on allocation of recent carbon: from beech leaves to soil CO₂ efflux, *New Phytologist*, 184, 950-961, 10.1111/j.1469-
842 8137.2009.03044.x, 2009.

843 Rukh, S., Sanders, T. G. M., Krüger, I., Schad, T., and Bolte, A.: Distinct [Responses of European Beech \(responses of](#)
844 [European beech \(L.\) to drought intensity and length - A review of the impacts of the 2003 and 2018-2019 drought events](#)
845 [in central Europe, Forests, 14, 10.3390/f14020248, 2023.](#)
846 ~~[L.\) to Drought Intensity and Length - A Review of the Impacts of the 2003 and 2018-2019 Drought Events in Central Europe,](#)~~
847 ~~[Forests, 14, ARTN-24810.3390/f14020248, 2023.](#)~~

848 Sabbatini, S., Mammarella, I., Arriga, N., Fratini, G., Graf, A., Hörtriagl, L., Ibrom, A., Longdoz, B., Mauder, M., Merbold,
849 L., Metzger, S., Montagnani, L., Pitacco, A., Rebmann, C., Sedlák, P., Sigut, L., Vitale, D., and Papale, D.: Eddy covariance
850 raw data processing for CO₂ and energy fluxes calculation at ICOS ecosystem stations, *International Agrophysics*, 32, 495-
851 +, 10.1515/intag-2017-0043, 2018.

Formatted: Left, Indent: Left: 0 cm, Hanging: 0.5 cm

Formatted: Left, Indent: Left: 0 cm, Hanging: 0.5 cm

Formatted: Left, Indent: Left: 0 cm, Hanging: 0.5 cm

Formatted: Indent: Left: 0 cm, Hanging: 0.5 cm

852 Schindlbacher, A., Wunderlich, S., Borken, W., Kitzler, B., Zechmeister-Boltenstern, S., and Jandl, R.: Soil respiration under
853 climate change: prolonged summer drought offsets soil warming effects, *Global Change Biology*, 18, 2270-2279,
854 10.1111/j.1365-2486.2012.02696.x, 2012.

855 Schultdt, B., Buras, A., Arend, M., Vitasse, Y., Beierkuhnlein, C., Damm, A., Gharun, M., Grams, T. E. E., Hauck, M., Hajek,
856 P., Hartmann, H., Hiltbrunner, E., Hoch, G., Holloway-Phillips, M., Körner, C., Larysch, E., Lübke, T., Nelson, D. B.,
857 Rammig, A., Rigling, A., Rose, L., Ruehr, N. K., Schumann, K., Weiser, F., Werner, C., Wohlgemuth, T., Zang, C. S., and
858 Kahmen, A.: A first assessment of the impact of the extreme 2018 summer drought on Central European forests, *Basic and*
859 *Applied Ecology*, 45, 86-103, 10.1016/j.baae.2020.04.003, 2020.

860 Schulze ED, B. E., Buchmann N, Clemens S, Müller-Hohenstein K, Scherer-Lorenzen M Springer (Ed.): *Plant Ecology*, 2,
861 928 pp, 2019.

862 Schwalm, C. R., Williams, C. A., Schaefer, K., Arneith, A., Bonal, D., Buchmann, N., Chen, J. Q., Law, B. E., Lindroth, A.,
863 Luysaert, S., Reichstein, M., and Richardson, A. D.: Assimilation exceeds respiration sensitivity to drought: A FLUXNET
864 synthesis, *Global Change Biology*, 16, 657-670, 10.1111/j.1365-2486.2009.01991.x, 2010.

865 Sendall, K. M., Reich, P. B., Zhao, C. M., Hou, J. H., Wei, X. R., Stefanski, A., Rice, K., Rich, R. L., and Montgomery, R. A.:
866 Acclimation of photosynthetic temperature optima of temperate and boreal tree species in response to experimental forest
867 warming, *Global Change Biology*, 21, 1342-1357, 10.1111/gcb.12781, 2015.

868 [Shapley, L. S.: Stochastic Games, P Natl Acad Sci USA, 39, 1095-1100, DOI 10.1073/pnas.39.10.1095, 1953.](#)

869 Shekhar, A., Humphrey, V., Buchmann, N., and Gharun, M.: More than three-fold increase of extreme dryness across Europe
870 by end of 21st century, 10.21203/rs.3.rs-3143908/v2, 2023.

871 Shekhar, A., Chen, J., Bhattacharjee, S., Buras, A., Castro, A. O., Zang, C. S., and Rammig, A.: Capturing the ~~Impaet~~**impact**
872 of the 2018 European ~~Drought~~**drought** and ~~Heat~~**heat** across ~~Different Vegetation Types Using~~**different vegetation types**
873 **using** OCO-2 Solar-Induced Fluorescence, Remote Sensing, 12, ~~ARTN 3249~~, 10.3390/rs12193249, 2020.

874 Shekhar, A., Hörtnagl, L., Paul-Limoges, E., Etzold, S., Zweifel, R., Buchmann, N., and Gharun, M.: Contrasting impact of
875 extreme soil and atmospheric dryness on the functioning of trees and forests, *Science of The Total Environment*,
876 [10.1016/j.scitotenv.2024.169931](#), 2024.

877 Smith, N. G. and Dukes, J. S.: Short-term acclimation to warmer temperatures accelerates leaf carbon exchange processes
878 across plant types, *Global Change Biology*, 23, 4840-4853, 10.1111/gcb.13735, 2017.

879 Sperlich, D., Chang, C. T., Peñuelas, J., and Sabaté, S.: Responses of photosynthesis and component processes to drought and
880 temperature stress: are Mediterranean trees fit for climate change?, *Tree Physiology*, 39, 1783-1805,
881 10.1093/treephys/tpz089, 2019.

882 Spinoni, J., Vogt, J. V., Naumann, G., Barbosa, P., and Dosio, A.: Will drought events become more frequent and severe in
883 Europe?, *International Journal of Climatology*, 38, 1718-1736, 10.1002/joc.5291, 2018.

884 [Strobl, C., Boulesteix, A.-L., Kneib, T., Augustin, T., and Zeileis, A.: Conditional variable importance for random forests,](#)
885 [BMC bioinformatics, 9, 1-11, 2008.](#)

Formatted: Indent: Left: 0 cm, Hanging: 0.5 cm

Formatted: Superscript

886 Sun, S. Q., Lei, H. Q., and Chang, S. X.: Drought differentially affects autotrophic and heterotrophic soil respiration rates and
887 their temperature sensitivity, *Biology and Fertility of Soils*, 55, 275-283, 10.1007/s00374-019-01347-w, 2019.

888 Talmon, Y., Sternberg, M., and Grünzweig, J. M.: Impact of rainfall manipulations and biotic controls on soil respiration in
889 Mediterranean and desert ecosystems along an aridity gradient, *Global Change Biology*, 17, 1108-1118, 10.1111/j.1365-
890 2486.2010.02285.x, 2011.

891 Team, R. C.: R: a language and environment for statistical computing. Vienna: R Foundation for Statistical Computing, (No
892 Title), 2021.

893 Trabucco, A.: Global aridity index and potential evapotranspiration (ET0) climate database v2, CGIAR Consort Spat Inf, 2019.

894 Tripathy, K. P. and Mishra, A. K.: How Unusual Is the 2022 European Compound Drought and Heatwave Event?, *Geophysical
895 Research Letters*, 50, ~~ARTN-e2023GL105453~~, 10.1029/2023GL105453, 2023.

896 van der Molen, M. K., Dolman, A. J., Ciais, P., Eglin, T., Gobron, N., Law, B. E., Meir, P., Peters, W., Phillips, O. L.,
897 Reichstein, M., Chen, T., Dekker, S. C., Doubkova, M., Friedl, M. A., Jung, M., van den Hurk, B. J. J. M., de Jeu, R. A.
898 M., Kruijt, B., Ohta, T., Rebel, K. T., Plummer, S., Seneviratne, S. I., Sitch, S., Teuling, A. J., van der Werf, G. R., and
899 Wang, G.: Drought and ecosystem carbon cycling, *Agricultural and Forest Meteorology*, 151, 765-773,
900 10.1016/j.agrformet.2011.01.018, 2011.

901 van der Woude, A. M., Peters, W., Joetzjer, E., Lafont, S., Koren, G., Ciais, P., Ramonet, M., Xu, Y. D., Bastos, A., Botia, S.,
902 Sitch, S., de Kok, R., Kneuer, T., Kubistin, D., Jacotot, A., Loubet, B., Herig-Coimbra, P. H., Loustau, D., and Lujikx, I.
903 T.: Temperature extremes of 2022 reduced carbon uptake by forests in Europe, *Nature Communications*, 14, ~~ARTN-6218~~,
904 10.1038/s41467-023-41851-0, 2023.

905 van Straaten, O., Veldkamp, E., and Corre, M. D.: Simulated drought reduces soil CO₂ efflux and production in a tropical
906 forest in Sulawesi, Indonesia, *Ecosphere*, 2, ~~Artn-119~~, 10.1890/Es11-00079.1, 2011.

907 von Buttlar, J., Zscheischler, J., Rammig, A., Sippel, S., Reichstein, M., Knohl, A., Jung, M., Menzer, O., Arain, M. A.,
908 Buchmann, N., Cescatti, A., Gianelle, D., Kiely, G., Law, B. E., Magliulo, V., Margolis, H., McCaughey, H., Merbold, L.,
909 Migliavacca, M., Montagnani, L., Oechel, W., Pavelka, M., Peichl, M., Rambal, S., Raschi, A., Scott, R. L., Vaccari, F. P.,
910 van Gorsel, E., Varlagin, A., Wohlfahrt, G., and Mahecha, M. D.: Impacts of droughts and extreme-temperature events on
911 gross primary production and ecosystem respiration: a systematic assessment across ecosystems and climate zones,
912 *Biogeosciences*, 15, 1293-1318, 10.5194/bg-15-1293-2018, 2018.

913 Wang, Y. F., Hao, Y. B., Cui, X. Y., Zhao, H. T., Xu, C. Y., Zhou, X. Q., and Xu, Z. H.: Responses of soil respiration and its
914 components to drought stress, *Journal of Soils and Sediments*, 14, 99-109, 10.1007/s11368-013-0799-7, 2014.

915 Wang, H., Yan, S. J., Ciais, P., Wigneron, J. P., Liu, L. B., Li, Y., Fu, Z., Ma, H. L., Liang, Z., Wei, F. L., Wang, Y. Y., and
916 Li, S. C.: Exploring complex water stress-gross primary production relationships: Impact of climatic drivers, main effects,
917 and interactive effects, *Global Change Biology*, 28, 4110-4123, 10.1111/gcb.16201, 2022.

Formatted: Indent: Left: 0 cm, Hanging: 0.5 cm

- 918 Wang, H., Yan, S. J., ~~Ciais~~Claiss, P., Wigneron, J. P., Liu, L. B., Li, Y., Fu, Z., Ma, H. L., Liang, Z., Wei, F. L., Wang, Y. Y.,
919 and Li, S. C.: Exploring complex water stress-gross primary production relationships: Impact of climatic drivers, main
920 effects, and interactive effects, *Global Change Biology*, 28, 4110-4123, 10.1111/gcb.16201, 2022.
- 921 Webb, E. K., Pearman, G. I., and Leuning, R.: Correction of Flux Measurements for Density Effects Due to Heat and Water-
922 Vapor Transfer, *Quarterly Journal of the Royal Meteorological Society*, 106, 85-100, DOI 10.1002/qj.49710644707, 1980.
- 923 ~~Wutzler, T., Lucas-Moffat, A., Migliavacca, M., Knauer, J., Sickel, K., Sigut, L., Menzer, O., and Reichstein, M.: Basic and~~
924 ~~extensible post-processing of eddy covariance flux data with REddyProc~~, *Biogeosciences*, 15, 5015-5030, 10.5194/bg-15-
925 ~~5015-2018, 2018~~.
- 926 Xu, B., Arain, M. A., Black, T. A., Law, B. E., Pastorello, G. Z., and Chu, H. S.: Seasonal variability of forest sensitivity to
927 heat and drought stresses: A synthesis based on carbon fluxes from North American forest ecosystems, *Global Change*
928 *Biology*, 26, 901-918, 10.1111/gcb.14843, 2020.
- 929 Yao, Y., Liu, Y. X., Zhou, S., Song, J. X., and Fu, B. J.: Soil moisture determines the recovery time of ecosystems from
930 drought, *Global Change Biology*, 29, 3562-3574, 10.1111/gcb.16620, 2023.
- 931 Zheng, P. F., Wang, D. D., Yu, X. X., Jia, G. D., Liu, Z. Q., Wang, Y. S., and Zhang, Y. G.: Effects of drought and rainfall
932 events on soil autotrophic respiration and heterotrophic respiration, *Agriculture Ecosystems & Environment*, 308, ~~ARTN~~
933 ~~407267~~, 10.1016/j.agee.2020.107267, 2021.
- 934 Zhou, S., Williams, A. P., Berg, A. M., Cook, B. I., Zhang, Y., Hagemann, S., Lorenz, R., Seneviratne, S. I., and Gentile, P.:
935 Land-atmosphere feedbacks exacerbate concurrent soil drought and atmospheric aridity, *Proceedings of the National*
936 *Academy of Sciences of the United States of America*, 116, 18848-18853, 10.1073/pnas.1904955116, 2019.

Formatted: Indent: Left: 0 cm, Hanging: 0.5 cm